Analyse d'images médicales pour les maladies cardiovasculaires

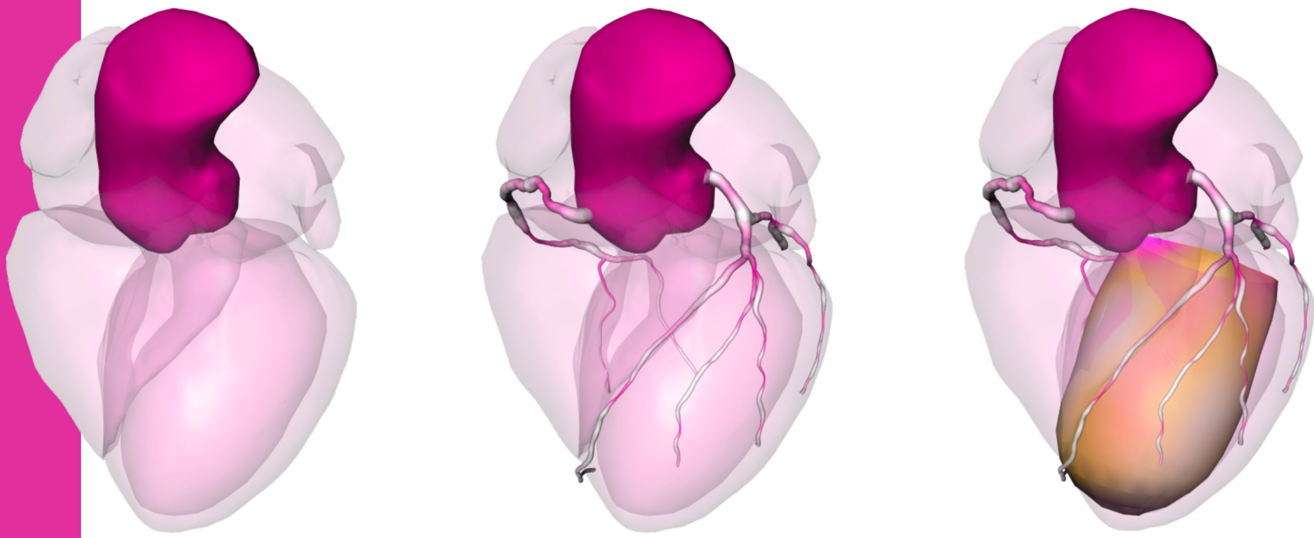

25 juin 2015
Workshop
VIVABRAIN
Paris, France

Dr. Hortense A. Kirisli
Project Manager / Advanced SW developer
AQUILAB, Lille, France

Cardiovascular anatomy quantification in CTA

Evaluation of a multi-atlas based method
for segmentation of cardiac CTA data:
a large-scale, multi-center and multi-vendor study

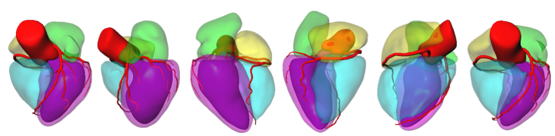

H.A. Kirişli, M. Schaap, S. Klein, S.L. Papadopoulou, M. Bonardi, C.H. Chen, A.C. Weustink,
N.R.A. Mollet, E.P.A. Vonken, R.J. van der Geest, T. van Walsum and W.J. Niessen,
Medical Physics, 37(12):6279–6292, 2010.

Cardiac segmentation
Purpose

- Functional information (ventricular mass, stroke volume, ejection fraction) extracted from CTA data is expected to improve the diagnostic value of the examination

- "If a robust cardiac segmentation method is provided, chamber and myocardial volumes derived from the segmentation results provide reliable functional measurements, and thus fully automatic analysis of four-chamber cardiac function can be achieved", Abadi et al., 2009.

- 3D cardiac models are useful for visualization and as region of interest for subsequent image analysis.

- → Investigate the accuracy and robustness of cardiac chamber delineation using a multi-atlas based segmentation method on multicenter and multivendor CTA data.

Cardiac segmentation
Method: multi-atlas based segmentation

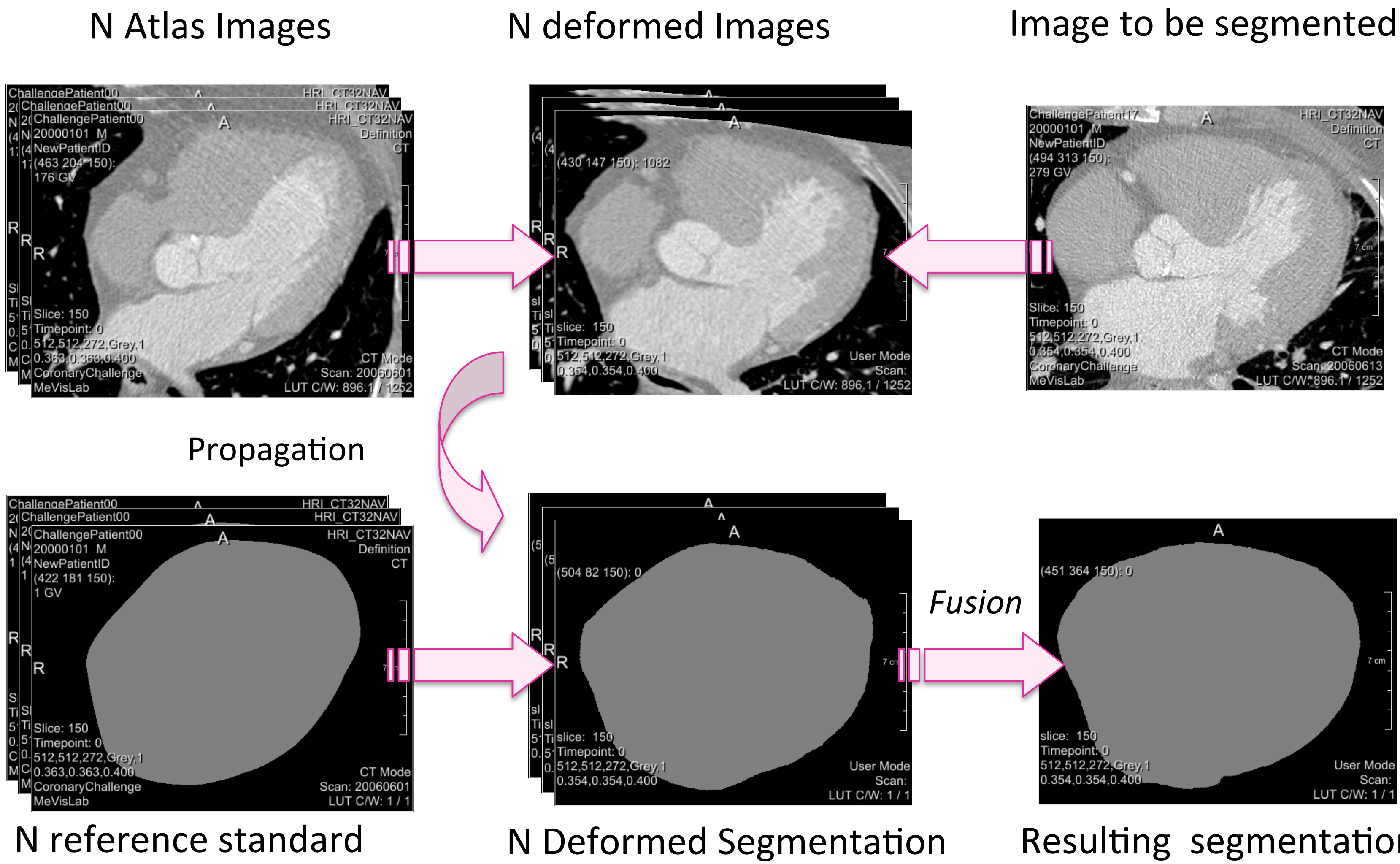

Cardiac segmentation
Method: multi-atlas based segmentation

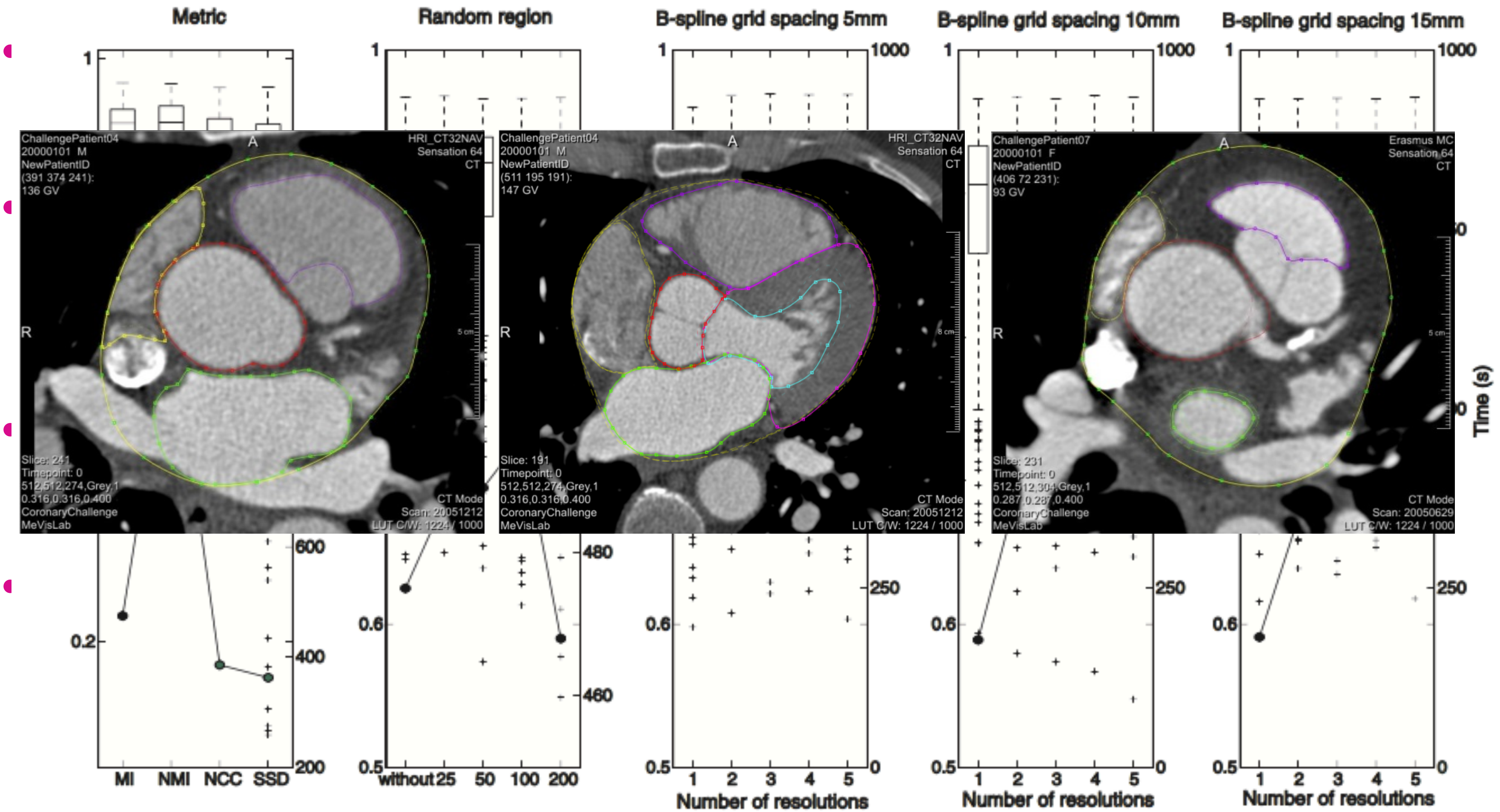

Cardiac segmentation

Datasets for large-scale multicenter multivendor evaluation

Table 2.1: multi-center/multi-vendor database used in the current evaluation study

Vendor	Scanner	Type	Institution	N_P (patients)	N_I (images)
SIEMENS	Somatom Definition	Dual-source	Erasmus MC, Rotterdam, The Netherlands	**795**	**1380**
PHILIPS			UMC Utrecht, Utrecht, The Netherlands	**20**	**20**
	Brillance iCT 256	256-slices		18	18
	Brillance 64	64-slices		2	2
GE	LightSpeed VCT	64-slices		**20**	**20**
			Centre Cardiologique du Nord, Paris, France	11	11
			Atlantic Medical Imaging, Galloway, NJ, USA	4	4
			Froedtert Hospital, Milwaukee, WI, USA	2	2
			Hong-Kong Sanatorium Hospital, Hong-Kong, China	2	2
			Keio University Hospital, Tokyo, Japan	1	1

Table 2.2 the
1380 imag b26f
smooth/b

Diasto

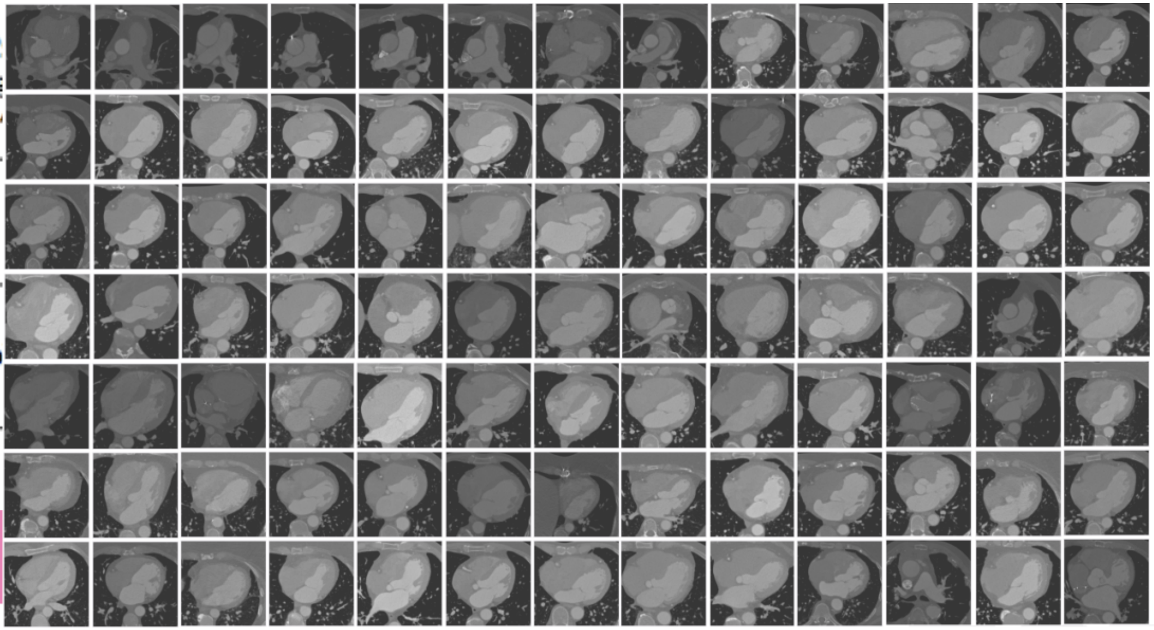

Cardiac segmentation
Evaluation framework

- 2D and 3D quantitative

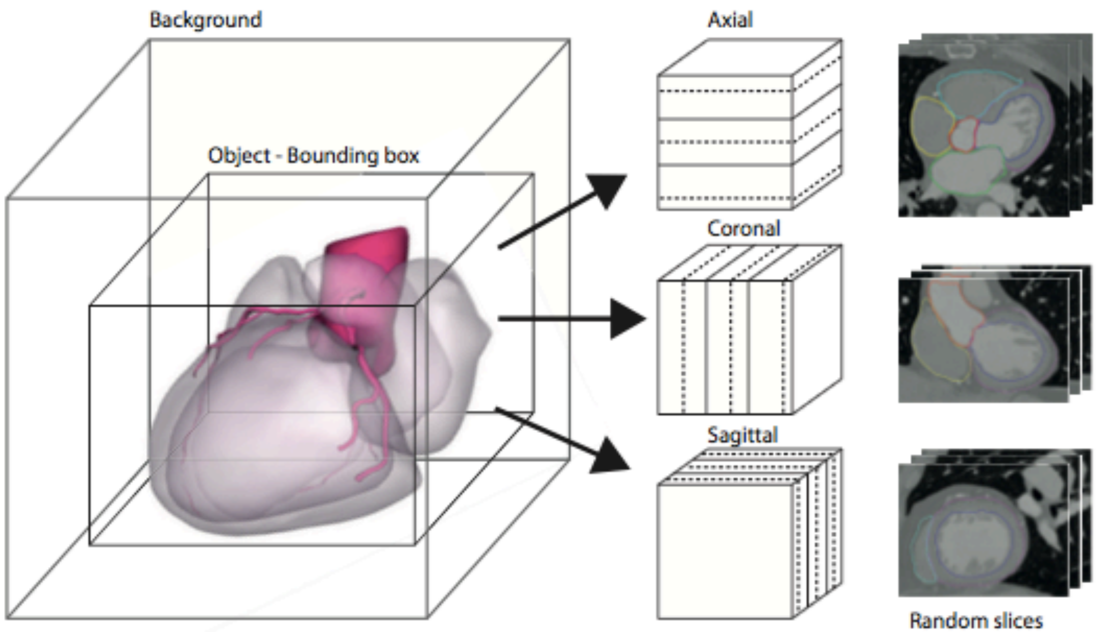

Figure 2.3: 2D quantitative evaluation. Random slice selection. A bounding box containing the object is calculated. This box is then divided into three sub-regions, in one direction (axial, sagittal or coronal), and one slice is randomly selected in each sub-region. This process is repeated for each of the three directions.

Cardiac segmentation
Evaluation framework

- 2D and 3D qualitative

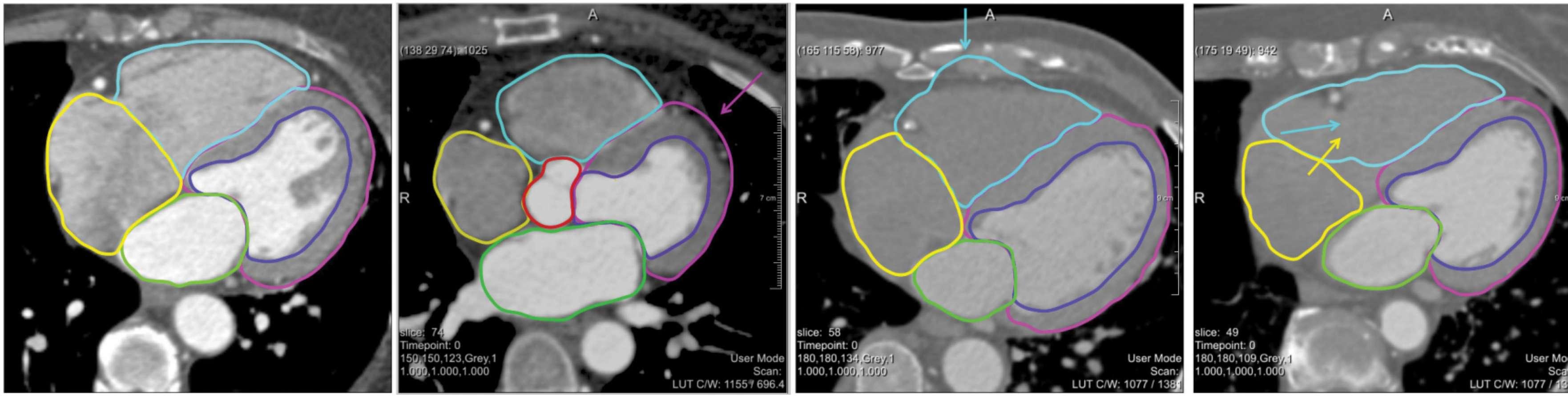

Table 2.3: Qualitative evaluation. Segmentation quality grade classification, published in Abadi et al. (2009). For each cardiac structure a separate grade is assigned. The term 'region' employed here refers to a certain part of a cardiac structure.

Grade	Description
1	Very accurate: Deviation up to 1mm
2	Most regions accurate: 1 or 2 regions may deviate up to 3mm
3	Most regions accurate: 1 region may deviate up to 1cm or more than 2 regions may deviate up to 3mm
4	A significant region (up to 50%) has not been segmented or has been incorrectly segmented
5	Segmentation failed

Table 2.4: Overview of the quantitative and qualitative evaluation. [a] see Section 2.6.1, [b] see Section 2.6.2 and [c] see Section 2.6.3 for more details.

		Quantitative		Qualitative	
Vendor	N	2D	3D	2D	3D
SIEMENS	8	-	Obs 1&2[a]	-	-
	20	Obs1[b]	-	Obs 1&2[c]	Obs 1&2[b,c]
	80	-	-	Obs 1&2[c]	Obs 1&2[c]
	1280	-	-	Obs2[c]	-
PHILIPS	20	Obs1[b]	-	-	Obs1[b]
GE	20	Obs1[b]	-	-	Obs1[b]

Cardiac segmentation

Results – 3D quantitative

Table 2.5: Experiment I : 8 cases leave-one-out study. Dice coefficient, mean surface-to-surface distance ± standard deviation, median, first quartile (Q1), third quartile (Q3), maximum distance (max). Distances are in millimeters (mm).

Structure	Dice	Mean ± stdev	Median	Q1	Q3	Max
Heart	0.96	0.99±1.25	0.72	0.30	1.69	9.20
epiLV	0.95	1.04±1.15	0.87	0.37	1.75	7.55
endoLV	0.95	0.62±0.63	0.60	0.35	1.08	4.92
RV	0.90	1.40±1.47	1.18	0.54	2.26	9.94
LA	0.94	0.66±0.84	0.53	0.29	1.06	6.77
RA	0.89	1.44±1.88	1.03	0.44	2.21	12.13
Ao	0.94	0.44±0.56	0.41	0.03	0.77	4.10

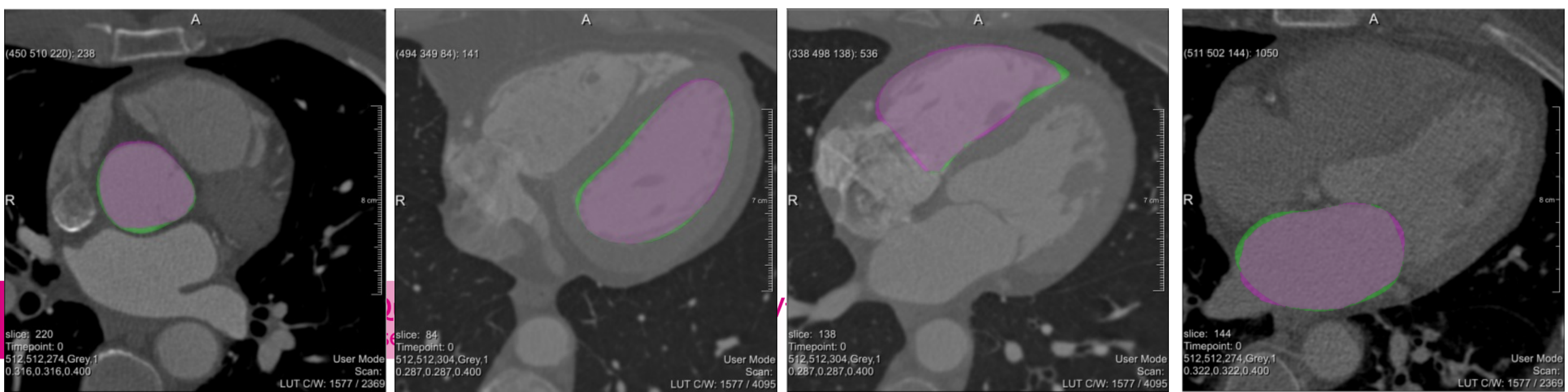

Cardiac segmentation
Results – 2D quantitative

Table 2.7: Experiment II: multi-center/multi-vendor study. 2D quantitative evaluation. For each image, cardiac contours are drawn by an expert on 5 randomly selected 2D slices (See Figure 2.3)), on axial, sagittal and coronal view. Comparison with the automatic segmentation: Dice coefficient, mean surface-to-surface distance ś standard deviation (in millimeters).

		N	Heart	epiLV	endoLV	RV	LA	RA	Ao	Mean
Dice	SIEMENS	20	0.93	0.94	0.94	0.89	0.94	0.89	0.92	0.92
	PHILIPS	20	0.91	0.91	0.92	0.90	0.91	0.88	0.91	0.90
	GE	20	0.89	0.91	0.92	0.87	0.88	0.86	0.89	0.89
Distance	SIEMENS	20	0.83±0.85	1.02±0.97	0.89±0.95	1.28±1.17	0.93±0.91	1.23±1.20	0.83±1.35	1.00±1.06
	PHILIPS	20	1.23±1.19	1.28±1.48	1.21±1.10	1.43±1.46	1.09±1.05	1.70±1.58	1.22±1.19	1.30±1.32
	GE	20	1.39±1.25	1.57±1.46	1.31±1.06	1.51±1.49	1.54±1.35	1.69±1.61	1.49±1.35	1.50±1.37

Cardiac segmentation

Results – 3D qualitative

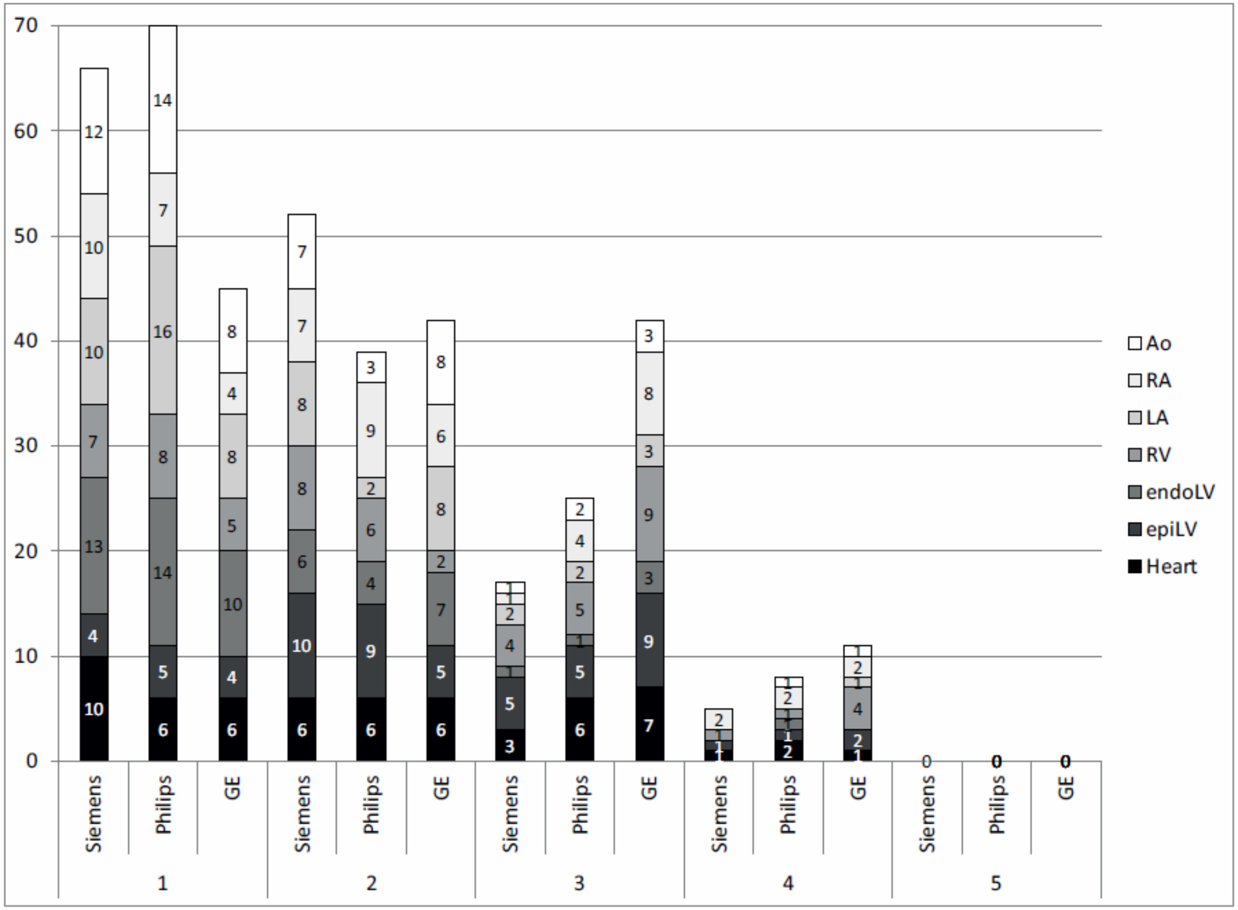

Figure 2.5: Experiment II: multi-center/multi-vendor study. 3D qualitative evaluation. Segmentations of the seven structures were visually checked by Obs1 and a grade was assigned (Table 2.3). Twenty patients were included per vendor. The numbers indicated in the bars correspond to the number of patient for who the segmentation of the structure has been assigned the grade.

Cardiac segmentation
Results – 3D qualitative

Figure 2.9: Experiment III: large-scale evaluation study. Examples of abnormal hearts. From left to right: left pneumonectomy, aortic aneurysm and congenital heart disease (transposition of great vessels).

Cardiac segmentation
Results – 3D qualitative

Table 2.9: Experiment III: large-scale study. 3D qualitative evaluation on 100 CTA data sets. Segmentations of the seven structures were visually checked by two observers (Obs1 & Obs2), and a grade was assigned (Table 2.3).

		Obs2				
	Grade	**1**	**2**	**3**	**4**	**5**
	1	30.0%	12.5%	0%	0%	0%
	2	9.0%	22.6%	7.0%	0%	0%
Obs1	**3**	0%	3.1%	8.8%	1.7%	0%
	4	0%	0%	1.5%	3.4%	0.1%
	5	0%	0%	0%	0%	0.3%

65% inter-observer agreement
74% grade 1&2
All in 1 category off

Cardiac segmentation

Results – 2D qualitative

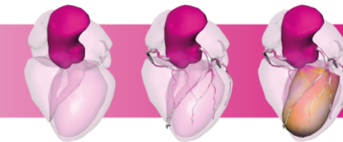

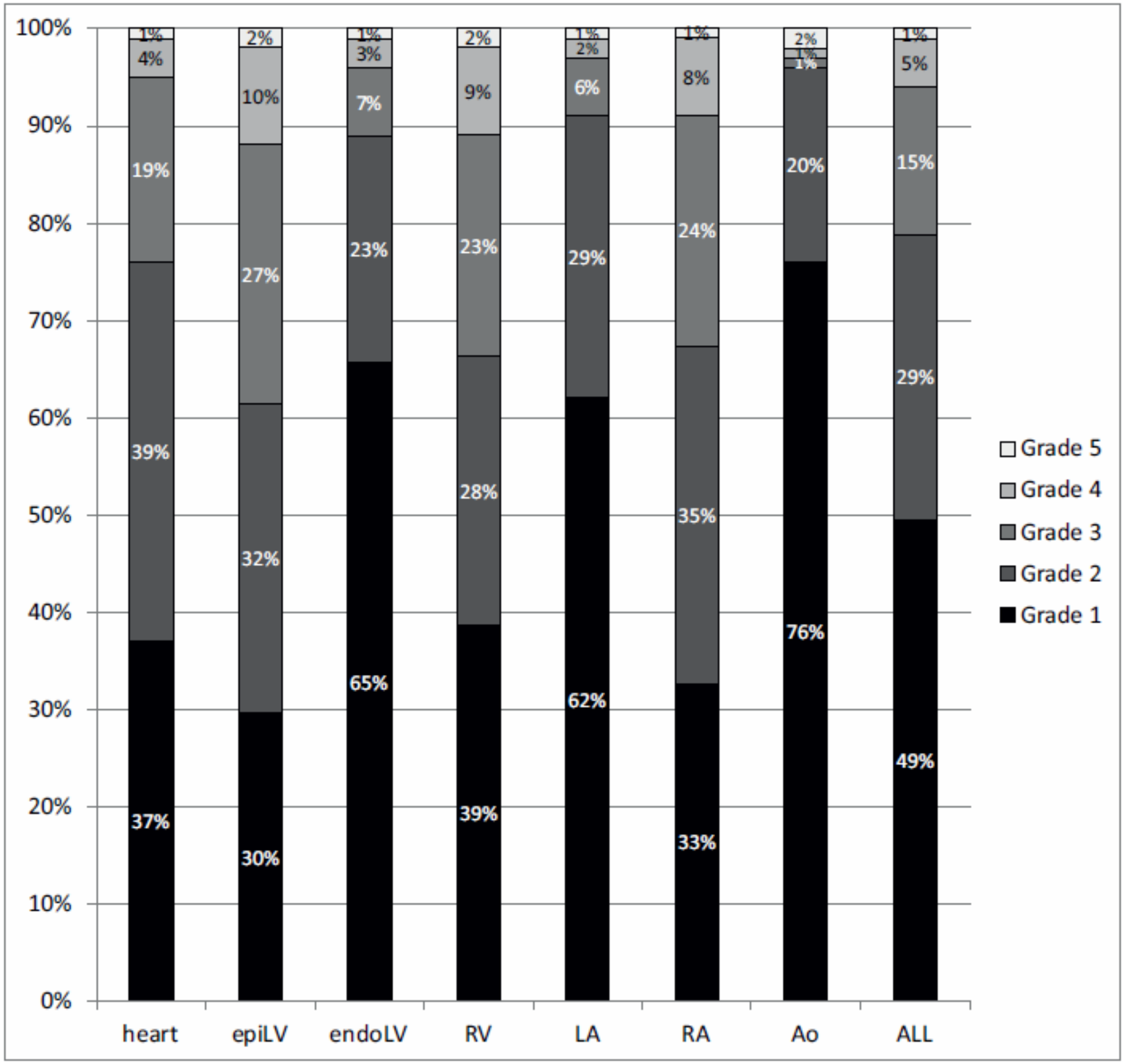

Figure 2.7: Experiment III: large-scale evaluation study. 2D qualitative evaluation on 1380 CTA data sets. Segmentations of the seven structures were visually checked in three orthogonal views (axial, coronal and sagittal), and a grade was assigned (Table 2.3).

Cardiac segmentation

Results – 2D qualitative

Table 2.8: Experiment III: large-scale study. 2D qualitative evaluation on 100 CTA data sets. Segmentations of the seven structures were visually checked in the three orthogonal views (axial, sagittal & coronal) by two observers (Obs1 & Obs2), and a grade was assigned (Table 2.3).

		Obs2				
	Grade	**1**	**2**	**3**	**4**	**5**
	1	48.6%	4.3%	0%	0%	0%
	2	9.9%	16.7%	4.0%	0%	0%
Obs1	**3**	0%	3.0%	7.6%	0.8%	0%
	4	0%	0%	0.2%	4.3%	0%
	5	0%	0%	0%	0%	0.6%

77% inter-observer agreement *(65% in 3D)*
79.5% in category 1&2 *(74% in 3D)*
All in one category off

Cardiac segmentation
Ways of improvement

- Atlas selection

Several novel atlas selection and atlas combination rules.

No ideal combination strategy; for each particular application, the best combination = trade-off accuracy and computational costs.

- Fusion method

"No combination algorithm is consistently better than the others for all images and all regions within the images"

"local weighting generally improved segmentation results"

Artaechevarria et al. (2009)

"Local weighted fusion algorithms yield better segmentations than global ones, and that weighted label fusion methods perform significantly better than majority voting"

Sabuncu et al. (2010)

Cardiac segmentation

- Conclusion

  Accurate delineation of cardiac chambers from CTA images can be achieved.
  (Chapter 2 of this thesis)

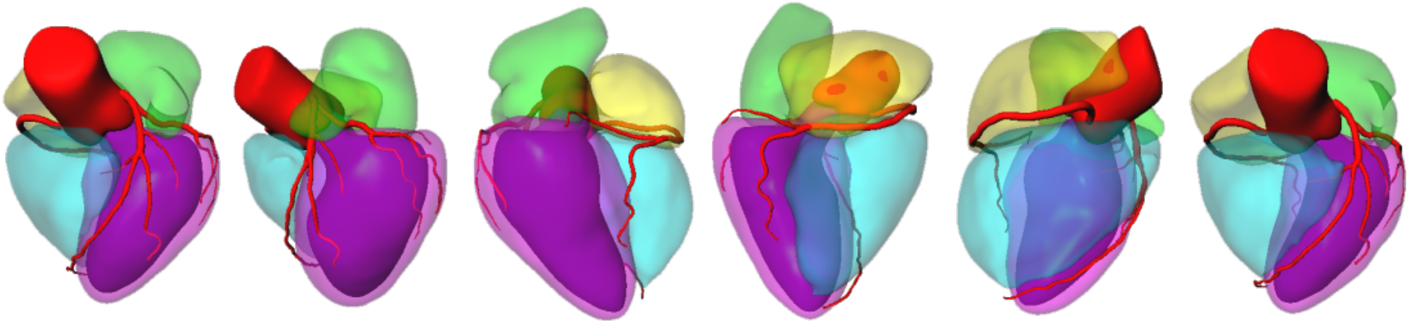

Cardiovascular anatomy quantification in CTA

Standardized evaluation framework
for evaluating coronary artery stenoses detection & quantification
and lumen segmentation algorithms
in Computed Tomography Angiography

H.A. Kirisli et al.,
Standardized evaluation framework for evaluating coronary artery stenosis detection, stenosis quantification and lumen segmentation algorithms in Computed Tomography Angiography,
Medical Image Analysis, 17(8):859-876, **2013**.

Rotterdam Coronary Artery Stenoses Algorithms Evaluation Framework

- GRAND CHALLENGES in medical image analysis
  - compare different algorithms for a particular task
  - on the same (clinically representative) data
  - using the same evaluation protocol

Compare different algorithms for a particular task…

Demonstrate the feasibility of dedicated (semi-)automatic algorithms for

- detection and quantification of stenosis
- coronary artery lumen segmentation

Rotterdam Coronary Artery Stenoses Algorithms Evaluation Framework

- GRAND CHALLENGES in medical image analysis
  - compare different algorithms for a particular task
  - on the same (clinically representative) data
  - using the same evaluation protocol

… on the same (clinically representative) data

48 DATASETS: 18 TRAINING + 30 TESTING

- Multi-center: Erasmus MC, LUMC, UMCU
- Multi-vendor: Siemens, Toshiba, Philips

Evaluation framework
Datasets

Table 4.1: Quantitative stenosis grading and stenosis types

Grade		Description
0	Normal	Absence of plaque and no luminal stenosis
1	Mild	Plaque with 20% - 49% stenosis
2	Moderate	Plaque with 50% - 69% stenosis
3	Severe	Plaque with 70% - 99% stenosis
4	Occluded	Complete occlusion of the lumen

Type	Description
Non-calcified	Plaque without calcium
Calcified	Plaque with $\geq$ 50% calcium
Mixed	Plaque with $\leq$ 50% calcium

Table 4.3: Distribution of patients (percentage of males) per coronary calcium score (CCS) category and per vendor. CCS refers to the Agatston score. The distribution of patients over the CCS categories was deduced from the work of Nieman et al. (2009), who reported on incidence of the different groups.

Center	Vendor	Scanner	CCS					
			0 *Low*	0.1-10 *Minimal*	11-100 *Mild*	101-400 *Moderate*	+400 *High*	Total N (% males)
EMC	SIEMENS	Somatom Definition	6 (100%)	1 (100%)	3 (80%)	4 (50%)	2 (50%)	16 (75%)
UMCU	PHILIPS	Brillance 64	3 (33%)	3 (66%)	5 (80%)	3 (33%)	2 (50%)	16 (56%)
LUMC	TOSHIBA	Aquilion ONE 320	2 (50%)	2 (0%)	6 (80%)	4 (75%)	2 (50%)	16 (68%)
		All	11 (72%)	6 (50%)	14 (78%)	11 (55%)	6 (50%)	48 (67%)

Evaluation framework
Datasets

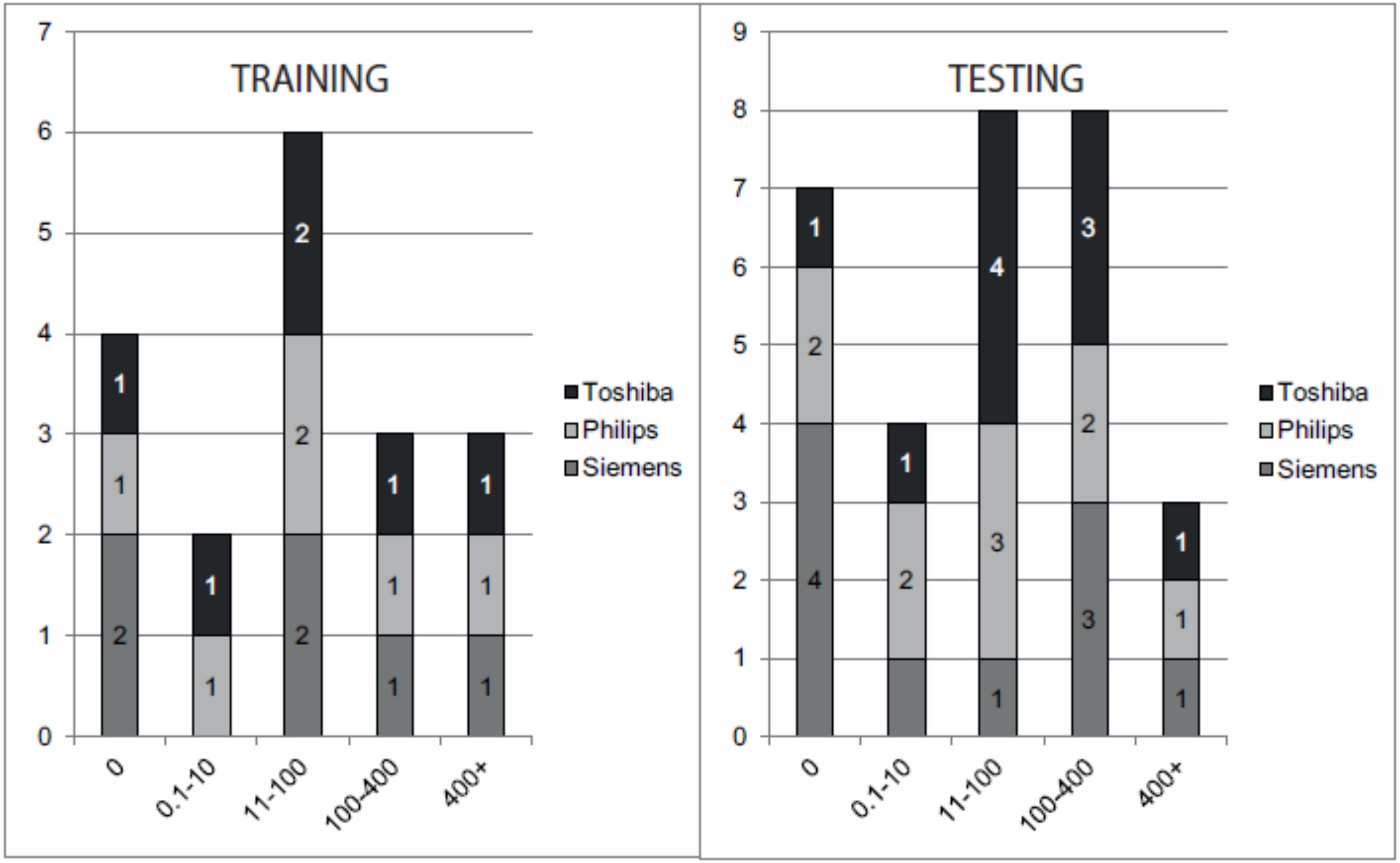

Figure 4.4: Distribution of 18 training and 30 testing datasets with respect to the different CCS categories and vendors.

Evaluation framework
Datasets

Table 4.5: Distribution of the coronary artery lesions ($\geq 20\%$) for the training and testing datasets. A lesion is considered as being significant if the luminal narrowing is $\geq 50\%$.

	Artery				
	RCA	LAD	LCX	IMB	All
Training					
CTA					
$\geq 20\%$	36	51	12	4	103
$\geq 50\%$	12	10	5	0	27
Testing					
CTA					
$\geq 20\%$	50	73	18	2	143
$\geq 50\%$	18	22	7	0	47

Evaluation framework
Datasets

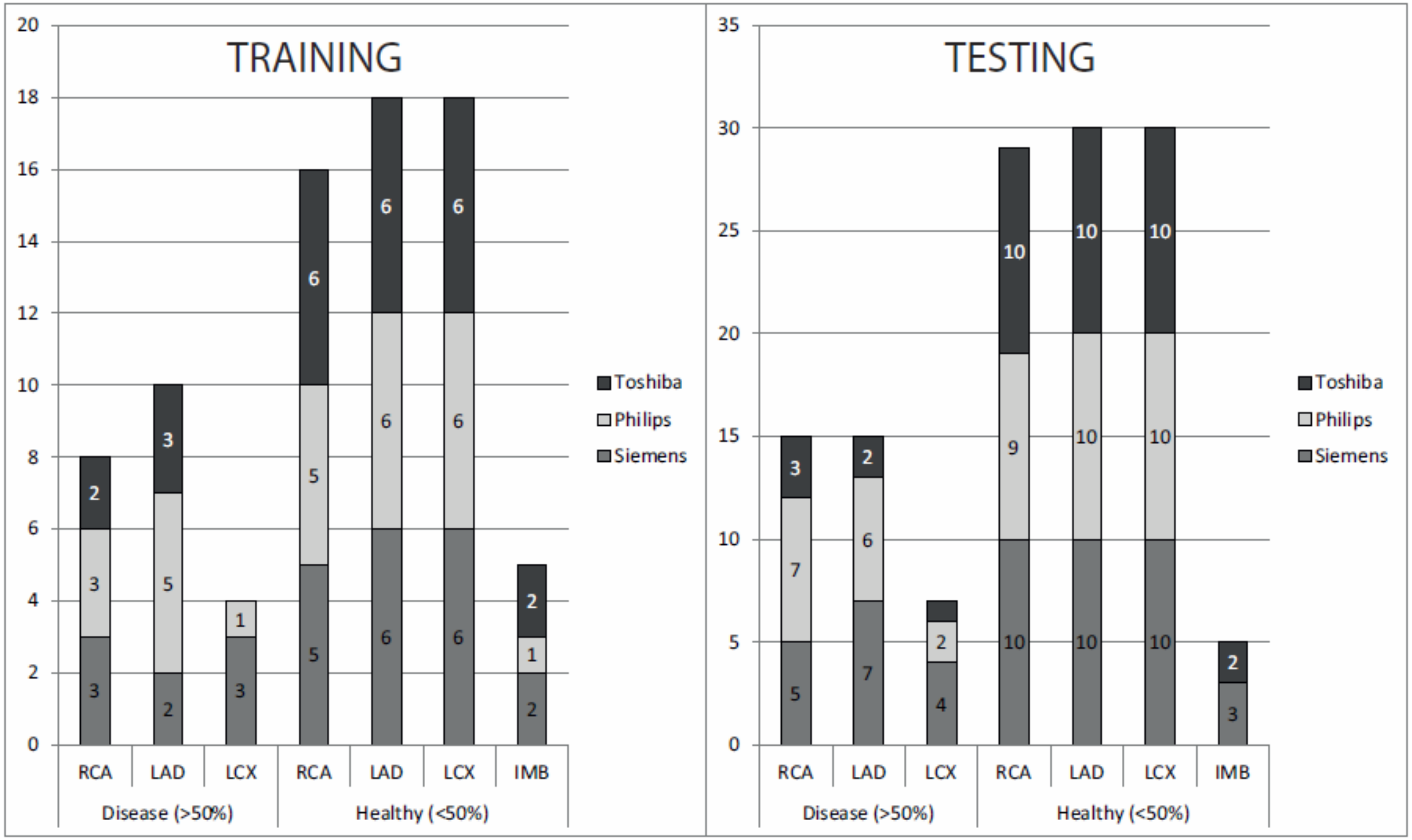

Figure 4.6: Overview of the segments considered for the lumen segmentation evaluation. *Diseased* segments are segments presenting in CTA consensus with at least one significant stenosis (≥50%). *Healthy* segments are segments presenting in CTA consensus with no significant stenosis (≤50%). Occluded segments were excluded from the lumen segmentation evaluation. The training set consists of 18 datasets and the testing set of 30 datasets.

Rotterdam Coronary Artery Stenoses Algorithms Evaluation Framework

- GRAND CHA
  - compa
  - on the
  - using t

… using the
  - QCA re
  - CTA cc
  - Clinica

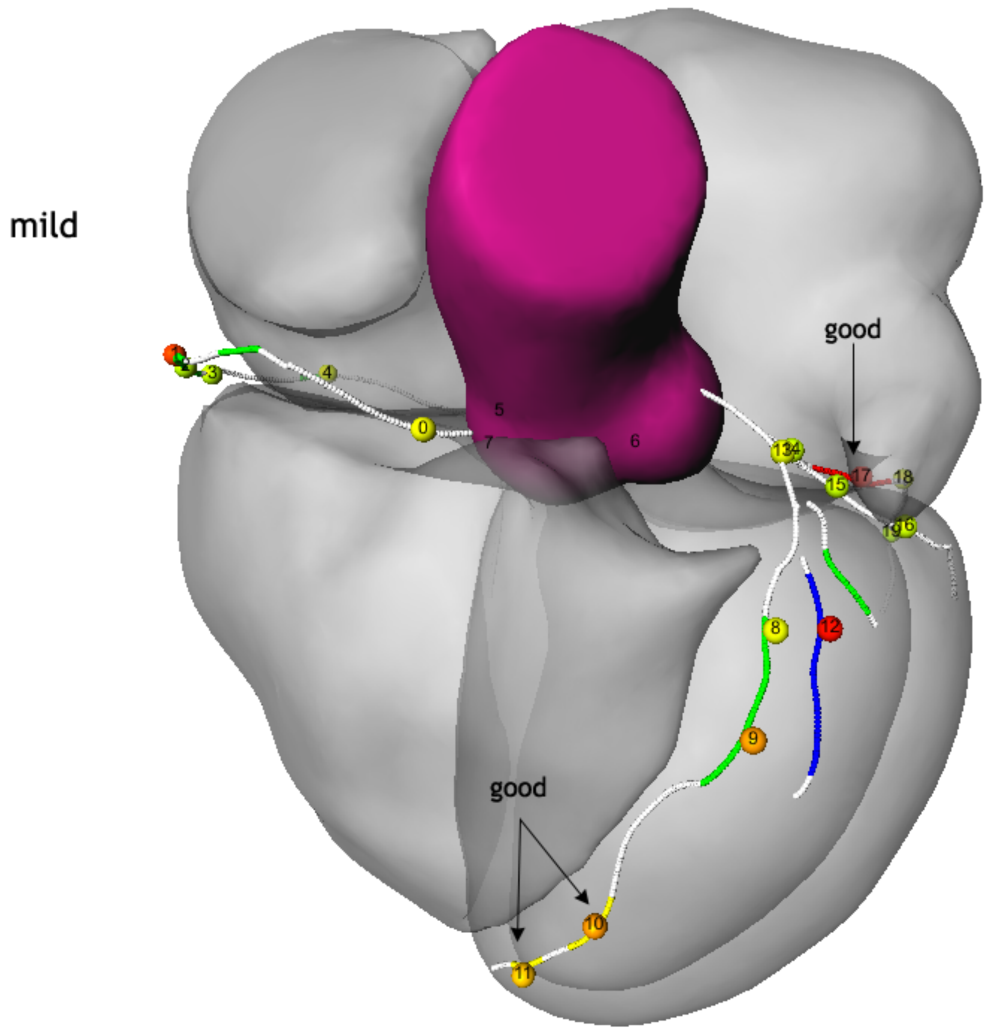

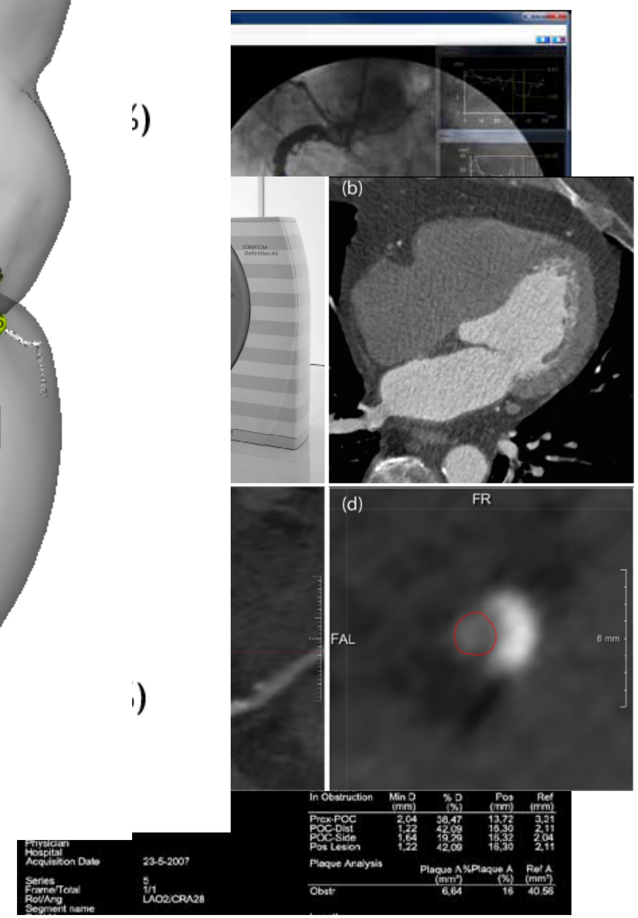

- Stenoses detection

Table 4.6: Stenosis detection, as compared to CTA and CCA reference standard. Descriptions of true-positive (TP), false-negative (FP), false-positive (FP) and true-negative (TN) detection.

$$R_D = \frac{1}{4} \cdot \left(\text{rank}^{CCA}_{Sens} + \text{rank}^{CCA}_{PPV} + \text{rank}^{CTA}_{Sens} + \text{rank}^{CTA}_{PPV}\right)$$

$$PPV = \frac{TP}{TP + FP} \quad (4.2)$$

D	
Tl	
Fl	
Fl	
Tl	
TP	
FN	
FP	
TN	No significant stenosis in a patient detected either by the reference standard and the algorithm.

Evaluation framework

Evaluation metrics

- Stenoses quantification

$$\sum_{i=1}^{S} \left| g^{i} - g^{i}_{ref} \right|$$

$$R_Q = \frac{1}{4} \cdot \left(\mathrm{rank}^{CCA}_{AAD} + \mathrm{rank}^{CCA}_{RMSD} + 2 \cdot \mathrm{rank}^{CTA}_{Kappa} \right)$$

$$RMSD = \sqrt{\frac{\cdots}{S}} \qquad (4.4)$$

Evaluation framework
Evaluation metrics

- Lumen segmentation

$$R_S = \frac{1}{N} \cdot \sum_{p=1}^{N} \left(\frac{\sum_{h=1}^{3} \mathrm{rank}_h^p}{3} + \omega^p \cdot \frac{\sum_{d=1}^{3} \mathrm{rank}_d^p}{3} \right)$$

Rotterdam Coronary Artery Stenoses Algorithms Evaluation Framework

- MICCAI'12 conference in Nice, France
- The algorithms from 11 research groups
- Open for new submissions
- 105 teams are active

http://coronary.bigr.nl/stenoses/

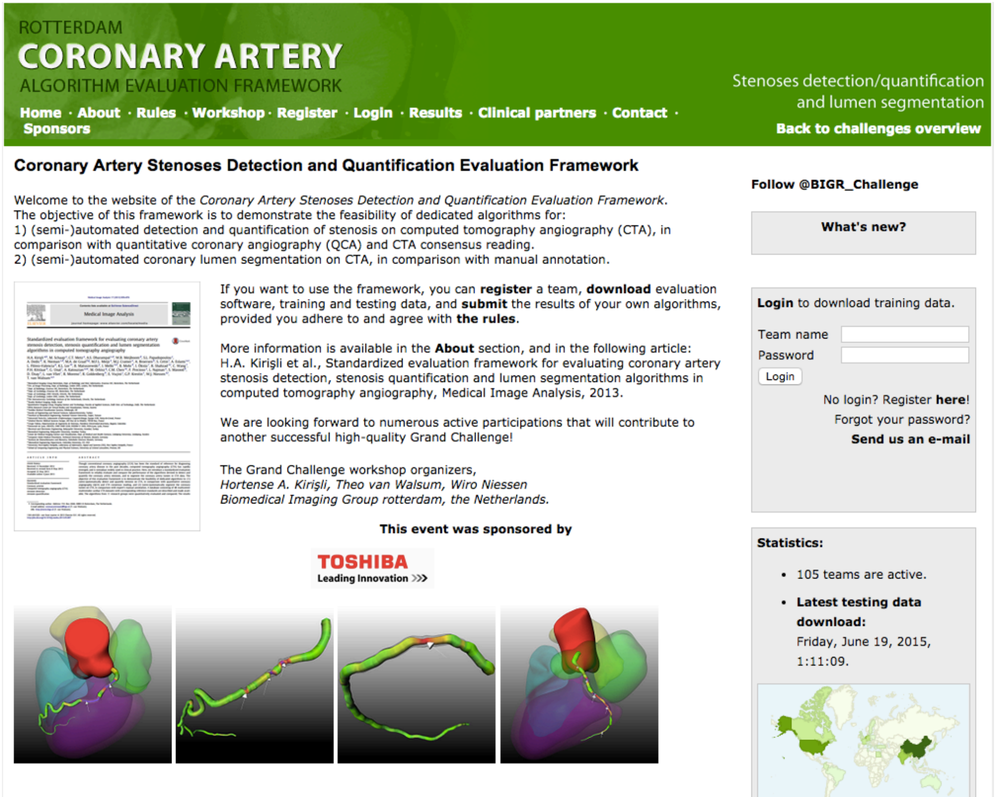

Evaluation framework

Results - Detection

Method	Cat.	QCA Sens. %	QCA Sens. rank	QCA P.P.V. %	QCA P.P.V. rank	CTA Sens. %	CTA Sens. rank	CTA P.P.V. %	CTA P.P.V. rank	Avg. rank
CTA Consensus	Min.User	82.1	2.0	52.3	1.0	100.0	1.0	100.0	1.0	1.2
Observer2	Min.User	75.0	3.0	51.2	2.0	70.2	3.0	80.5	2.0	2.5
Observer1	Min.User	85.7	1.0	40.0	5.0	83.0	2.0	60.9	3.0	2.8
Observer3	Min.User	64.3	5.0	42.9	4.0	66.0	4.0	59.6	4.0	4.2
Cetin et al. Vessel intensity & geometric features	Min.User	53.6	10.0	19.2	11.0	53.2	6.0	26.0	9.0	9.0
Mohr et al. Level-sets & tissue classification	Automatic	57.1	7.0	14.4	13.0	51.1	7.0	15.7	13.0	10.0
Wang et al. Level-sets	Automatic	25.0	16.0	50.0	3.0	10.6	19.0	33.3	5.0	10.8
Melki et al. Learning based detection	Automatic	57.1	7.0	11.3	17.0	55.3	5.0	11.5	14.0	10.8
Eslami et al. Likelihood	Min.User	67.9	4.0	9.4	18.0	51.1	7.0	4.0	18.0	11.8
Broersen et al. LKEB	Automatic	25.0	16.0	18.9	12.0	27.7	15.0	31.0	7.0	12.5
Duval et al. Feature extraction	Automatic	57.1	7.0	12.2	15.0	42.6	12.0	7.6	16.0	12.5
Shahzad et al. Int J Card Img	Min.User	28.6	15.0	24.2	8.0	21.3	16.0	23.3	12.0	12.8
Öksüz et al. Region growing	Min.User	21.4	18.0	22.2	9.0	17.0	17.0	25.8	10.0	13.5
Melki et al. Watershed	Automatic	46.4	13.0	12.1	16.0	42.6	12.0	9.3	15.0	14.0
Lor et al. Probabilistic	Min.User	50.0	12.0	13.9	14.0	31.9	14.0	3.0	19.0	14.8
Flórez-Valencia et al. Kalman filter	Min.User	17.9	19.0	8.5	19.0	14.9	18.0	4.8	17.0	18.2

Evaluation framework

Results - Quantification

Method	Cat.	QCA Avg. Abs. diff. %	QCA Avg. Abs. diff. rank	QCA R.M.S. diff. %	QCA R.M.S. diff. rank	CTA Weigthed Kappa K	CTA Weigthed Kappa rank	Avg. rank
CTA Consensus	Min.User	28.8	2.0	34.4	2.0	1.00	1.0	1.5
Observer1	Min.User	30.1	3.0	35.2	3.0	0.74	3.0	3.0
Observer2	Min.User	31.1	7.0	36.5	4.0	0.77	2.0	3.8
Observer3	Min.User	30.6	4.0	36.9	6.0	0.73	4.0	4.5
Wang et al. Level-sets	Automatic	28.8	1.0	33.7	1.0	0.18	11.0	6.0
Shahzad et al. Int J Card Img	Min.User	31.0	6.0	39.3	8.0	0.29	8.0	7.5
Broersen et al. LKEB	Automatic	32.5	8.0	39.3	7.0	0.27	9.0	8.2
Öksüz et al. Region growing	Min.User	47.0	10.0	53.1	10.0	0.21	10.0	10.0
Lor et al. Probabilistic	Min.User	38.6	9.0	42.7	9.0	-0.03	15.0	12.0
Mohr et al. Level-sets & tissue classification	Automatic	49.6	12.0	56.0	15.0	0.15	12.0	12.8
Eslami et al. Likelihood	Min.User	50.9	14.0	55.0	11.0	-0.02	14.0	13.2
Flórez-Valencia et al. Kalman filter	Min.User	51.6	15.0	55.6	13.0	0.01	13.0	13.5

Evaluation framework

Results - Segmentation

Method	Cat.	DICE *diseased*		DICE *healthy*		MSD *diseased*		MSD *healthy*		MAXSD *diseased*		MAXSD *healthy*		Avg. rank
		%	rank	%	rank	mm	rank	mm	rank	mm	rank	mm	rank	
Observer3	Min.User	0.79	2.0	0.81	1.9	0.23	2.6	0.21	2.1	3.00	7.8	3.45	7.0	3.9
Observer1	Min.User	0.76	3.0	0.77	4.6	0.24	3.2	0.24	3.9	2.87	6.8	3.47	7.0	4.8
Mohr et al. **Level-sets & tissue classification**	Automatic	0.70	5.8	0.73	5.2	0.40	6.4	0.39	5.3	2.68	4.1	2.75	3.0	4.9
Observer2	Min.User	0.65	7.6	0.72	7.1	0.34	7.2	0.27	5.5	2.82	6.9	3.26	6.5	6.7
Shahzad et al. **Int J Card Img**	Min.User	0.65	8.5	0.68	7.9	0.39	8.2	0.41	7.2	2.73	6.1	3.20	4.8	7.0
Wang et al. **Level-sets**	Automatic	0.69	6.7	0.69	6.7	0.45	8.0	0.55	8.0	3.94	7.7	6.48	8.3	7.6
Broersen et al. **LKEB**	Automatic	0.67	7.1	0.69	7.2	0.50	8.4	0.70	8.5	3.89	7.7	5.86	7.9	7.8
Flórez-Valencia et al. **Kalman filter**	Min.User	0.42	10.9	0.38	10.8	0.83	10.2	1.13	10.5	3.81	5.9	6.96	8.0	9.5

Evaluation framework
Results

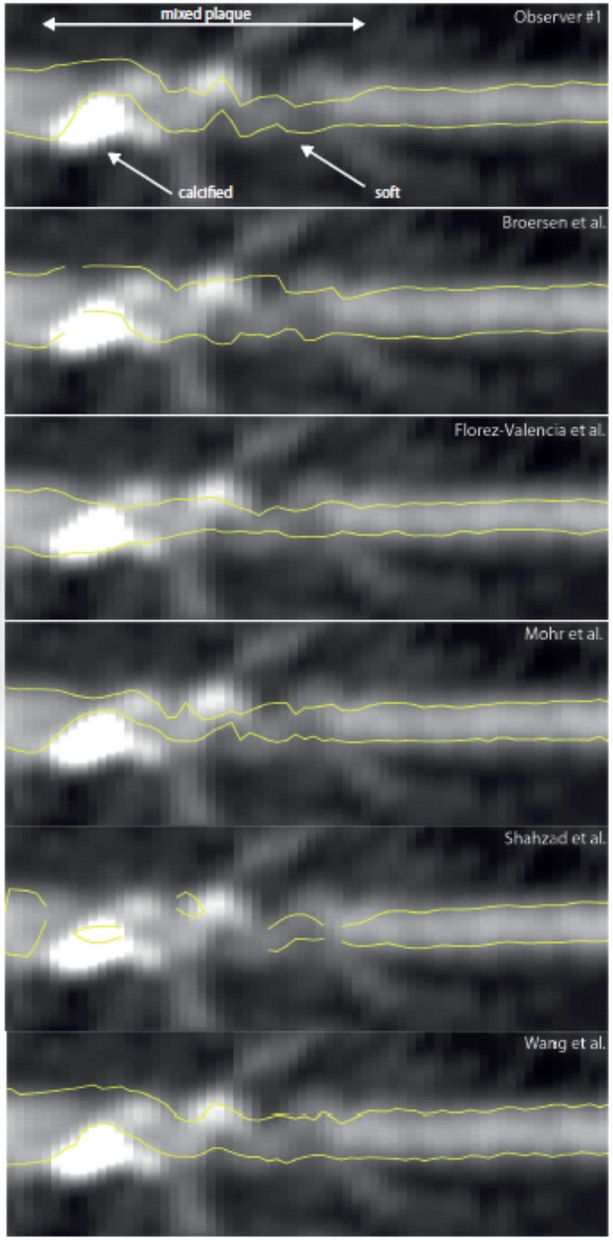

Figure 4.10: Lumen segmentation example for training dataset #08. Visual impression of the reference standard of observer#1 and evaluated algorithms of Broersen et al., Flórez Valencia et al., Mohr et al., Shahzad et al., and Wang et al.. Dataset #08 presents a severe mixed plaque in segment LAD7. Note that for this particular view of the vessel, the method of Shahzad et al. and Broersen et al. fail to display segmentation at some vessel position; in fact, their segmentation lies in another plane, and thus, no intersection was available.

Rotterdam Coronary Artery Stenoses Algorithms Evaluation Framework

- MICCAI'12 conferenc in Nice, France
- The algorithms from 1 research groups
- Open for new submissions
- 105 active teams

CONCLUSIONS *(Chapter 3*

http://coronary.bigr.nl/stenoses/

Coronary artery lumen segme

?

Coronary artery stenoses dete

- ✗ used stand-alone in
- ✓ used as a second-rea

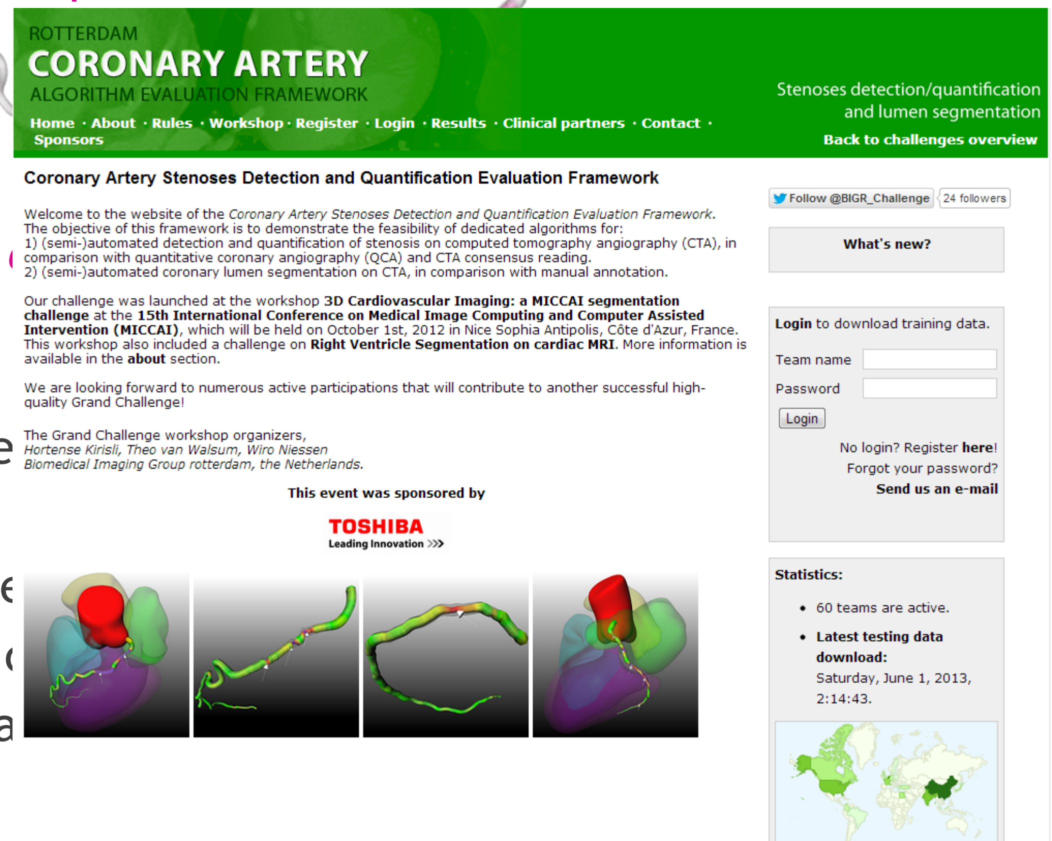

Cardiovascular anatomy quantification in CTA

Automatic Detection and Quantification of Coronary Artery Stenoses using Contrast Enhanced Cardiac CT Scans

R. Shahzad*, H.A. Kirişli*, C. Metz, H. Tang, M. Schaap, W.J. Niessen, L. van Vliet and T. van Walsum

*both authors contributed equally to this research,

International Journal of Cardiovascular Imaging, 29:1-13, 2013

Detection of stenoses on CTA

Method

- Centerline extraction:

C. Metz et al. “Coronary centerline extraction from CT coronary angiography images using a minimum cost path approach”. Medical Physics 36 (12), 5568–5579, 2009

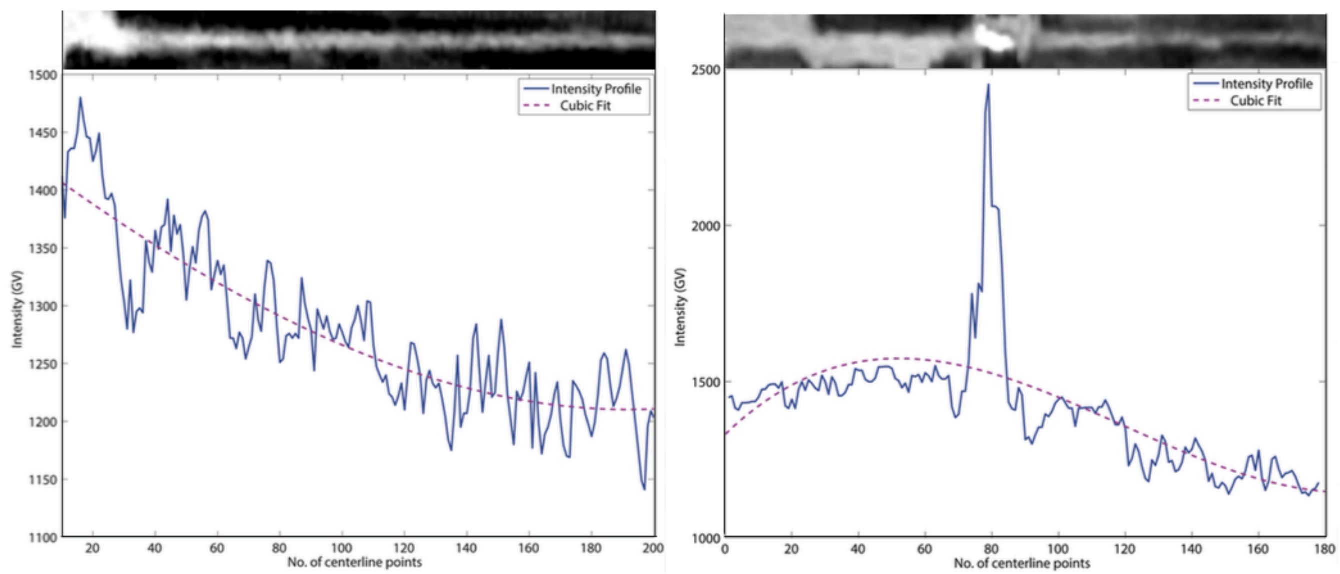

Figure 3.1: Intensity profiles through two coronary arteries, presenting (a) no calcium objects (b) a high density calcium object.

Detection of stenoses on CTA
Method

- Centerline refinement: calcium removal

$$I(x) - F(x)|_{x \in X} \geq T_{ca}$$

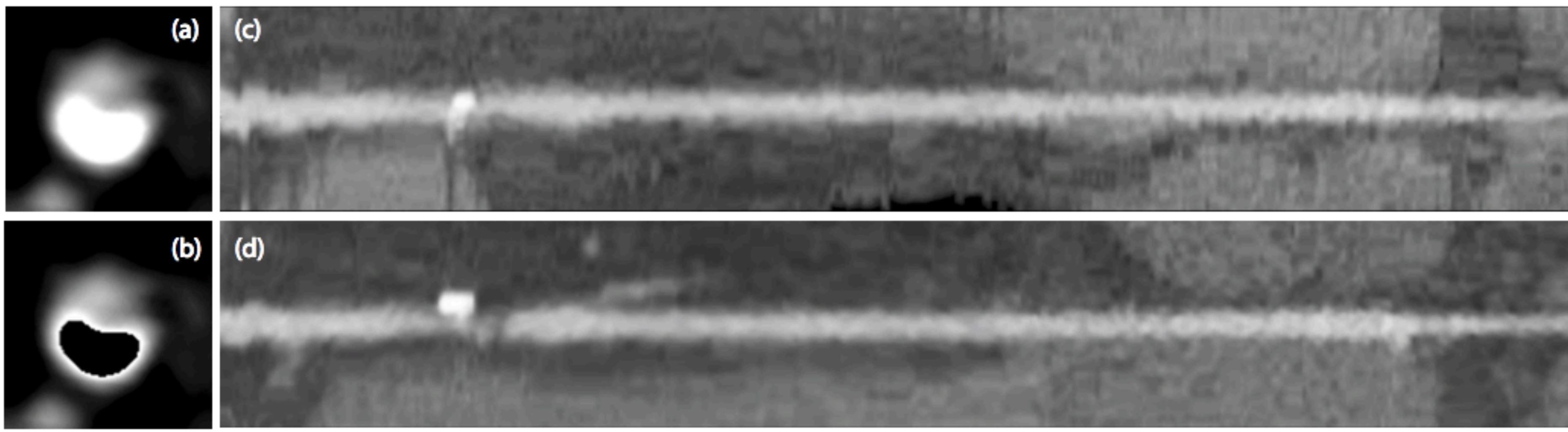

Figure 3.2: A random cross-sectional image slice through a calcium lesion (a) before and (b) after calcium suppression. CMPR image (c) before and (d) after refinement.

Detection of stenoses on CTA
Method

- Bifurcation detection:

  T. van Walsum et al. « Averaging centerlines: mean shift on paths”.
  In: Proc. of the 11th international conference on Medical Image Computing and Computer Assisted Intervention (MICCAI’08). Vol. 11. Springer, pp. 900–907., 2008.

$$x_{kl}^{\tau+1} = \frac{\sum_{i,j} c_{kl,ij}\,\phi_{kl,ij}\,G\left(x_{kl}^{\tau}|x_{ij},\sigma\right)x_{ij}}{\sum_{i'j'} c_{kl,i'j'}\,\phi_{kl,i'j'}\,G\left(x_{kl}^{\tau}|x_{i'j'},\sigma\right)}$$

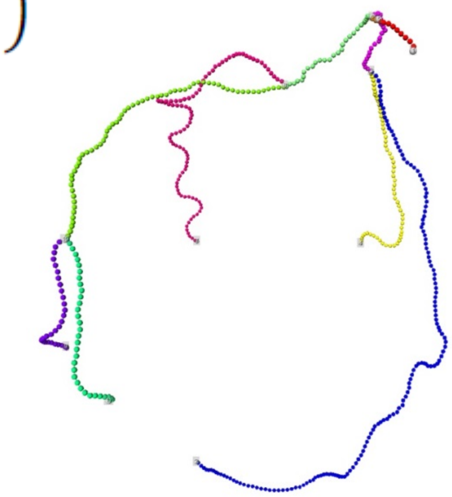

Detection of stenoses on CTA
Method

- Lumen segmentation:

M. Schaap et al., “Coronary lumen segmentation using graph cuts and robust kernel regression”. In Proc. of Information Processing in Medical Imaging (IPMI). pp. 528–539, 2009

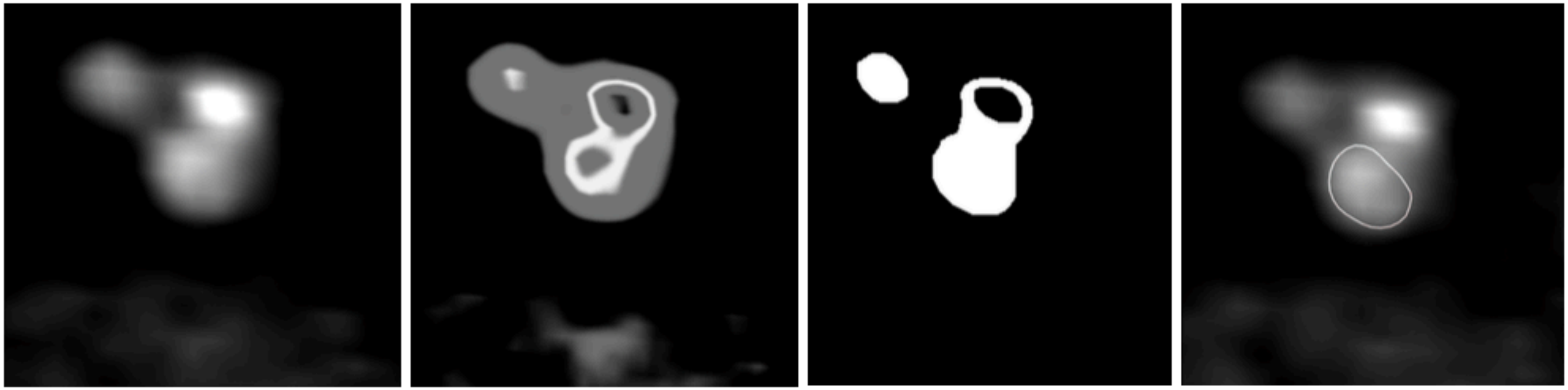

Figure 3.3: A MPR image of a vessel, with visible calcium lesion and side branch (a) Original image (b) Resulting image after segmentation (c) Binarized segmented image after graph-cuts (lumen bright, background black) (d) Resulting lumen segmentation after robust kernel regression.

- Stenosis detection and quantification:

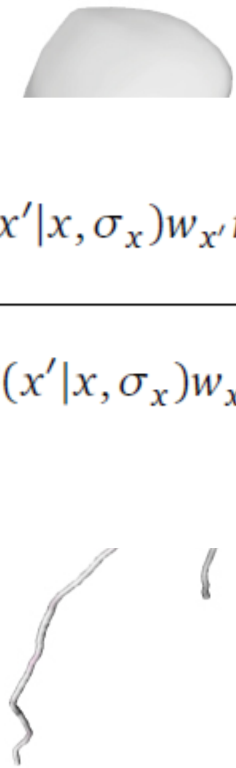

$$\hat{r}_x = \frac{\sum_{x'=1}^{N} G(x'|x,\sigma_x) w_{x'} r_{x'}}{\sum_{x'=1}^{N} G(x'|x,\sigma_x) w_{x'}}$$

$$(3.5) \quad \begin{cases} w_x = G(r_x | r_x^{max}, \sigma_r) \\ r_x^{max} = \dfrac{\sum_{x'=1}^{N} G(x'|x,\sigma_{max}) r_{x'}}{\sum_{x'=1}^{N} G(x'|x,\sigma_{max})} \\ G(x'|x,\sigma) = \dfrac{1}{\sigma\sqrt{2\pi}} e^{-\frac{(x'-x)^2}{2\sigma^2}} \end{cases}$$

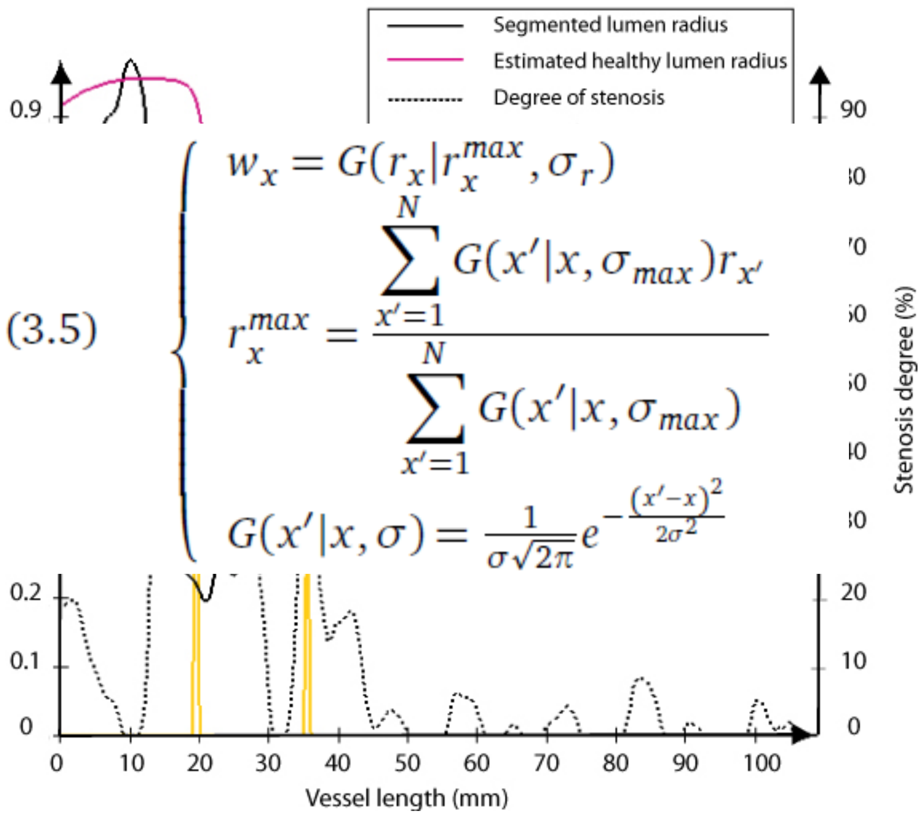

Detection of stenoses on CTA

Results

- Training data / Parameter optimization

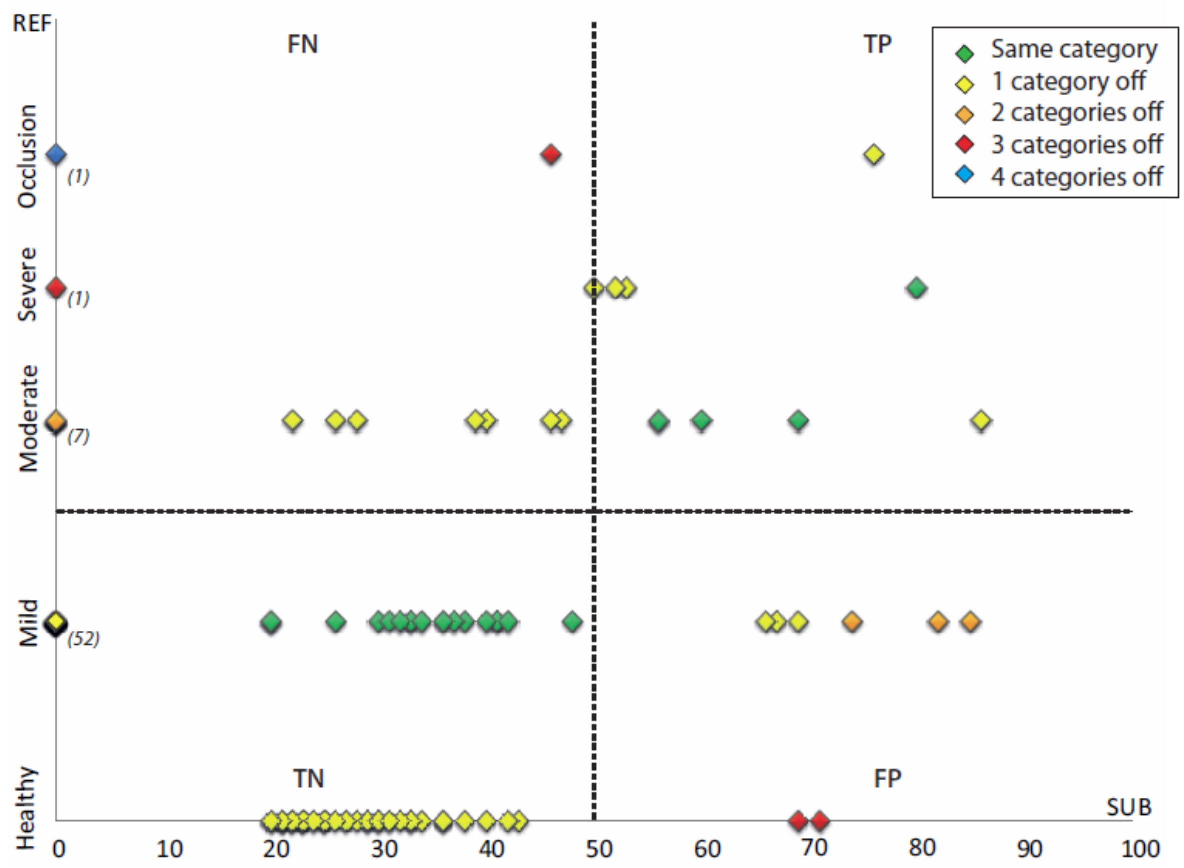

Figure 3.5: Stenoses detection and quantification - Results obtained on the 18 training datasets after optimization of the parameters: 90% of the stenoses detected with our new method are quantified with an error of one grade or less (yellow and green detections).

Detection of stenoses on CTA
Results

- Testing data

Table 3.1: Detection - Our method's performances are compared with the observers' ones.

(%)	Training				Testing			
Method	QCA		CTA		QCA		CTA	
	Sens.	*PPV*	*Sens.*	*PPV*	*Sens.*	*PPV*	*Sens.*	*PPV*
Observer 1	72	49	92	57	86	40	83	61
Observer 2	76	66	82	73	75	51	70	81
Observer 3	52	68	63	74	64	43	66	60
Our method	48	63	37	56	29	24	21	23

Table 3.2: Quantification - Our method's performances are compared with the observers' ones.

	Training			Testing		
Method	QCA		CTA	QCA		CTA
	Abs Diff (%)	*RMS diff (%)*	*Weighted* κ	*Abs Diff (%)*	*RMS diff (%)*	*Weighted* κ
Observer 1	29.7	35.1	0.71	30.1	35.2	0.74
Observer 2	25.5	31.8	0.84	31.1	36.5	0.77
Observer 3	29.1	35.1	0.73	30.6	36.9	0.73
Our method	26.3	34.8	0.37	31.0	39.3	0.29

Detection of stenoses on CTA

Results

- Testing data

Table 3.3: Segmentation - Our method's performances are compared with the observers' ones. Diseased (D) / Healthy (H) segments.

	Training						Testing					
Method	Dice (%)		MSD (mm)		MAXSD (mm)		Dice (%)		MSD (mm)		MAXSD (mm)	
	D	*H*	*D*	*H*	*D*	*H*	*D*	*H*	*D*	*H*	*D*	*H*
Observer 1	74	79	0.26	0.26	3.29	3.61	76	77	0.24	0.24	2.87	3.47
Observer 2	66	73	0.31	0.25	2.70	3.00	64	72	0.34	0.27	2.82	3.26
Observer 3	76	80	0.24	0.19	3.07	3.25	79	81	0.23	0.21	3.00	3.45
Our method	66	70	0.37	0.32	2.49	3.04	65	68	0.39	0.41	2.73	3.20

Detection of stenoses on CTA

Results

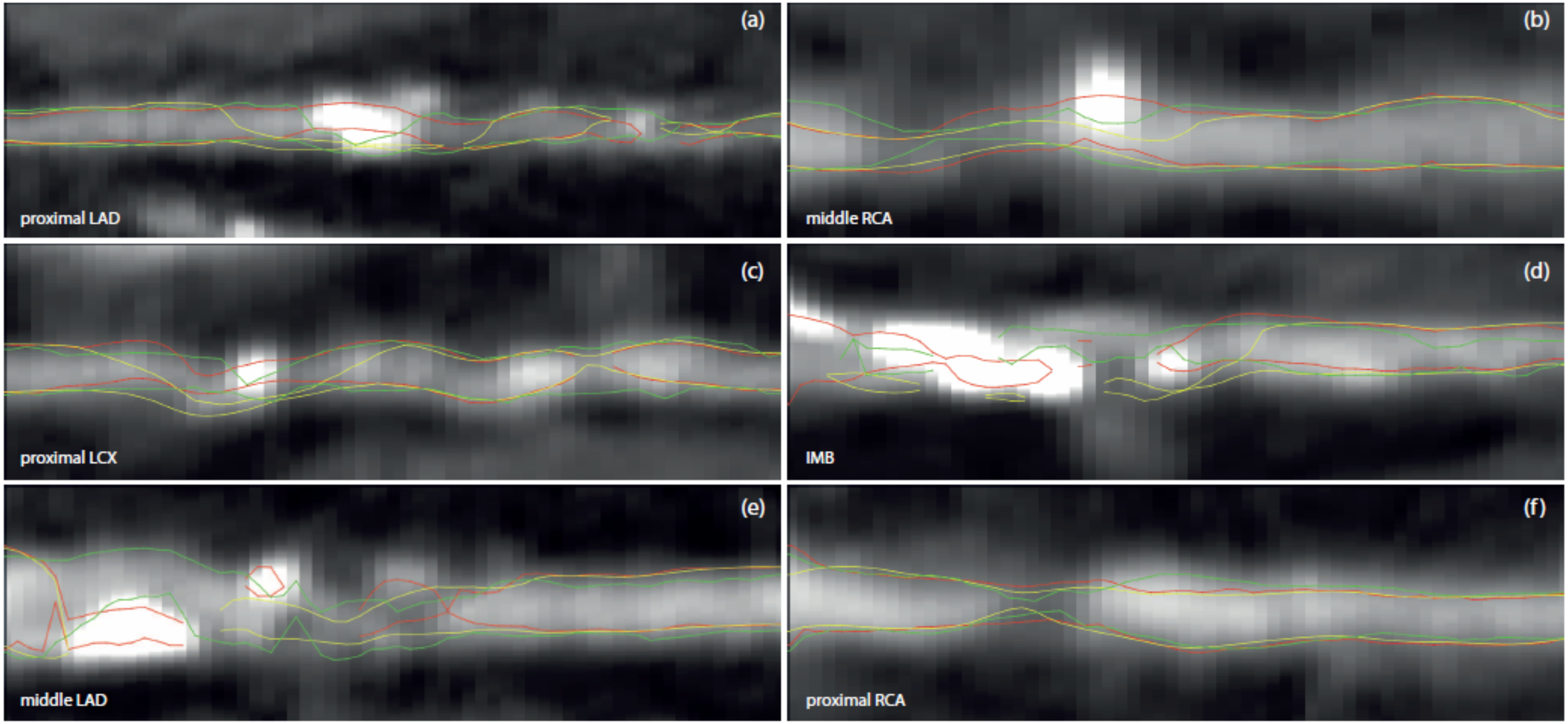

Figure 3.6: Coronary artery lumen segmentation examples. Our previous method (method without the calcium suppression step in the centerline refinement) (red), our method (yellow), one of the observer (green). (a)(b)(c) Cases where our method (with the calcium suppression step in the centerline refinement) achieves segmentation similar to the observer. (d) Case where the method avoid the calcified plaque; however, the observer segmented the other side of the plaque. (e) Case where issue with large calcified plaque remains. (f) Example of segmentation of a coronary segment presenting a soft plaque.

Fused visualization of cardiac anatomical and functional information

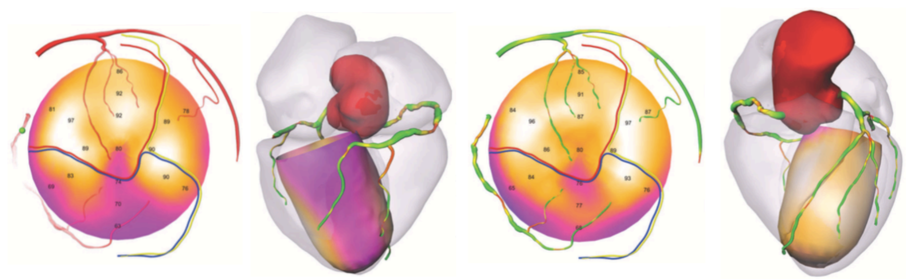

Additional diagnostic value of fused cardiac CTA and SPECT analysis: a multi-center evaluation study using the Synchronized Multimodal heART Visualization (SMARTVis) system

H.A. Kirisli, V. Gupta, R. Shahzad, I. Al Younis, A. Dharampal, R-J.M. van Geuns, A. Scholte, M.A. de Graaf, R.M.S. Joemai, K. Nieman, L. van Vliet, T. van Walsum, B.P.F. Lelieveldt and W.J. Niessen, Journal of Nuclear Medicine, 55(1):50-57, 2014.

SMARTVis
Clinical workflow

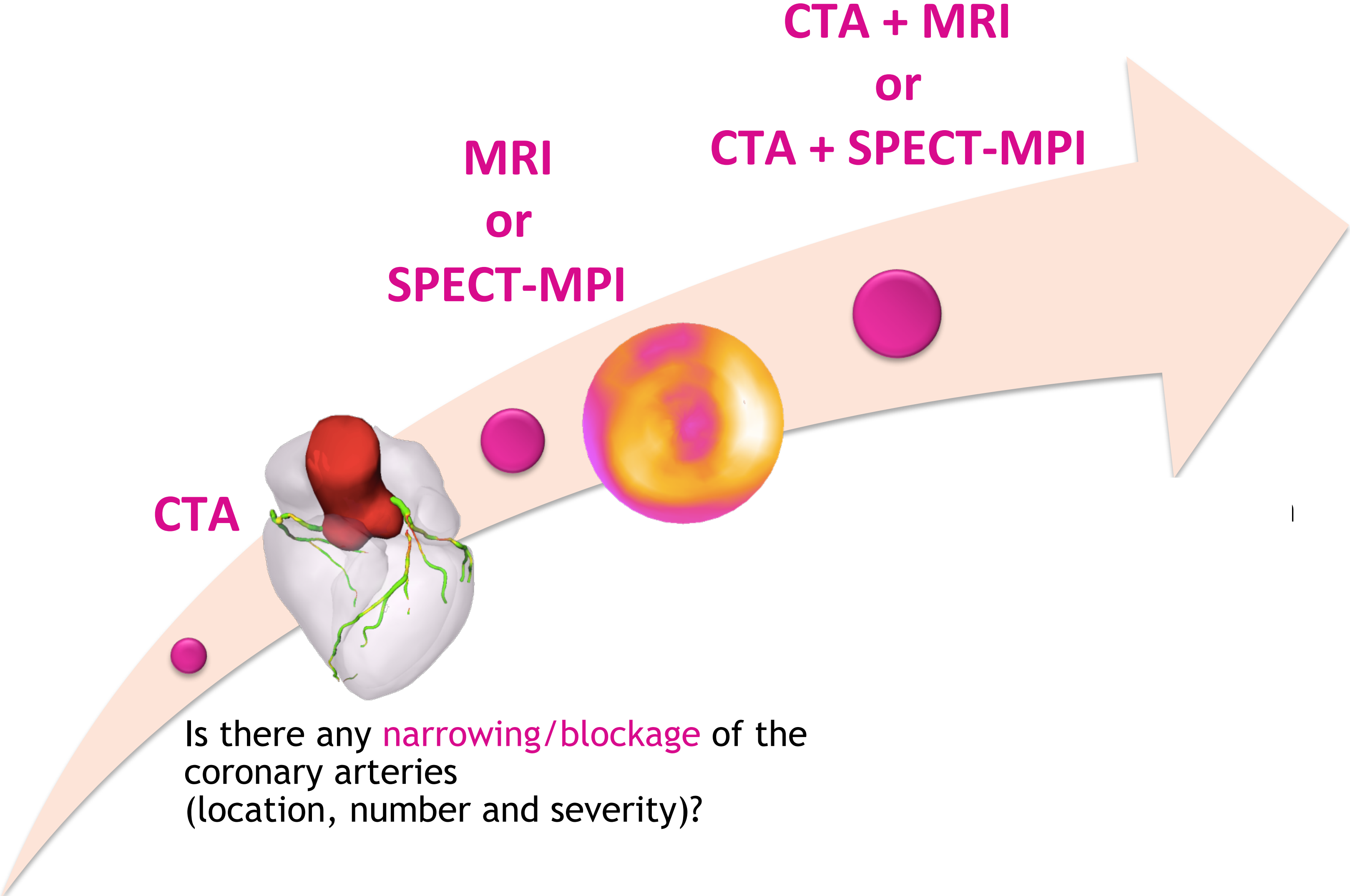

Is there any narrowing/blockage of the coronary arteries
(location, number and severity)?

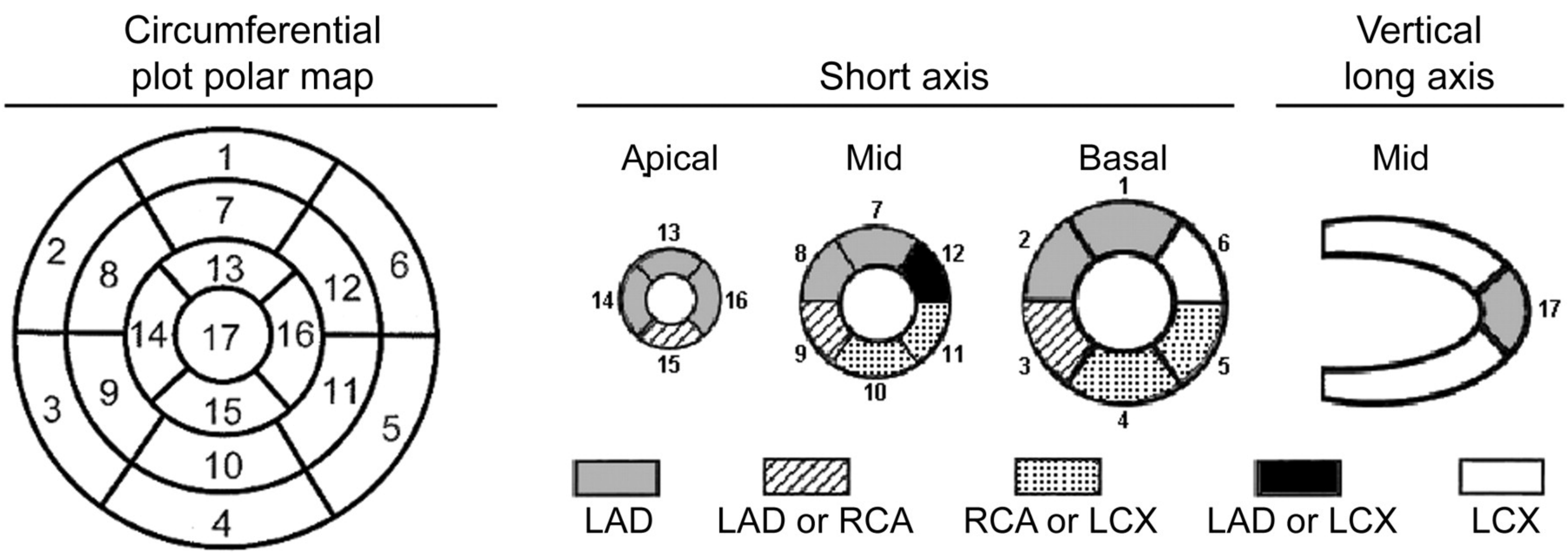

1. Basal anterior
2. Basal anteroseptal
3. Basal inferoseptal
4. Basal inferior
5. Basal inferolateral
6. Basal anterolateral
7. Mid-anterior
8. Mid-anteroseptal
9. Mid-inferoseptal
10. Mid-inferior
11. Mid-inferolateral
12. Mid-anterolateral
13. Apical anterior
14. Apical septal
15. Apical inferior
16. Apical lateral
17. Apex

- **Coronary artery perfusion territories**
  Territoires de perfusion des artères coronaires / Koroner perfüzyon toprakları

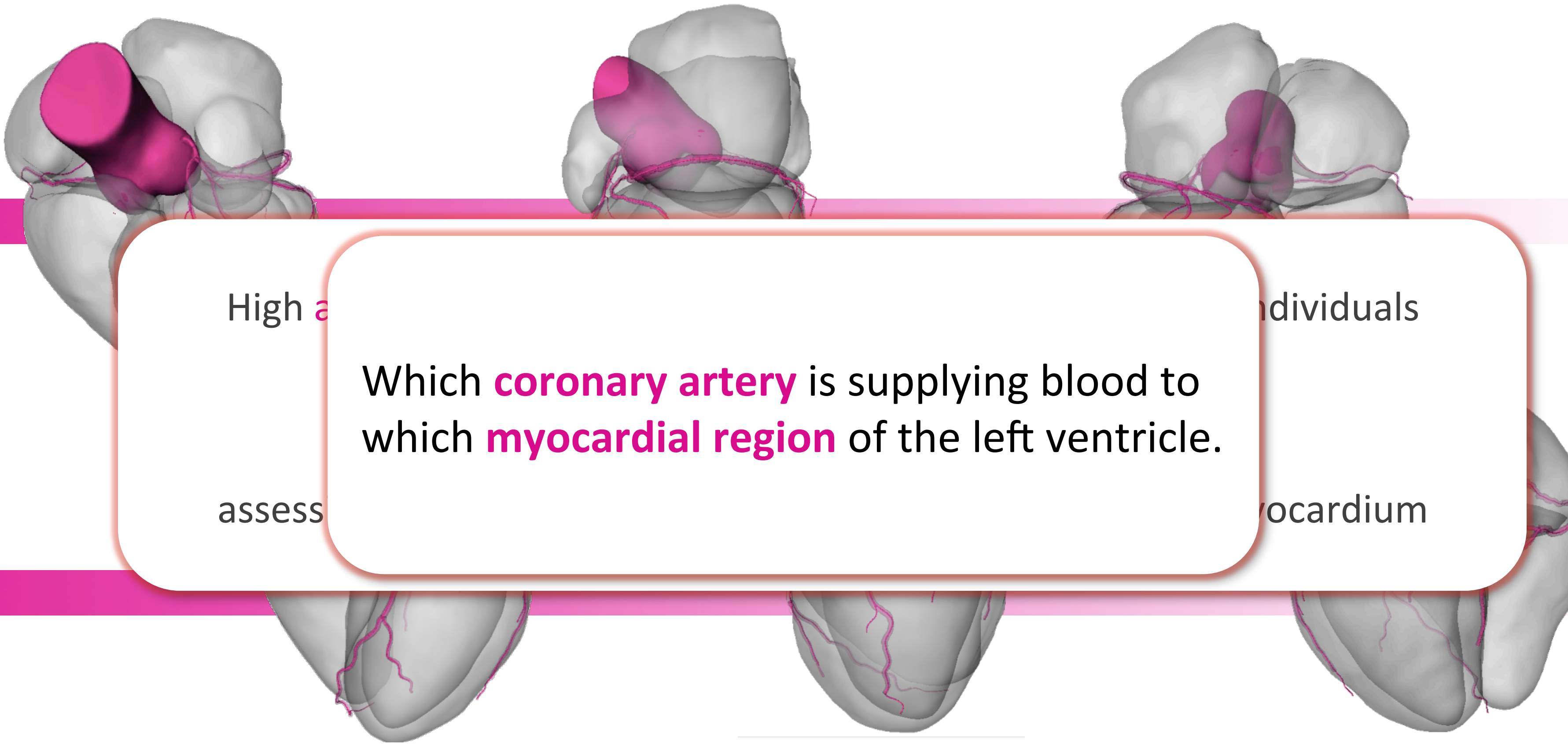

High a ndividuals

Which **coronary artery** is supplying blood to which **myocardial region** of the left ventricle.

assess ocardium

SMARTVis

A better way to diagnose CAD

- 2D and 3D models
- Integrate anatomical information to 2D functional polar maps
- Integrate functional information with 3D coronary anatomy
- Color-code degree of stenosis, automatic detection,…
- 2D and 3D model synchronization

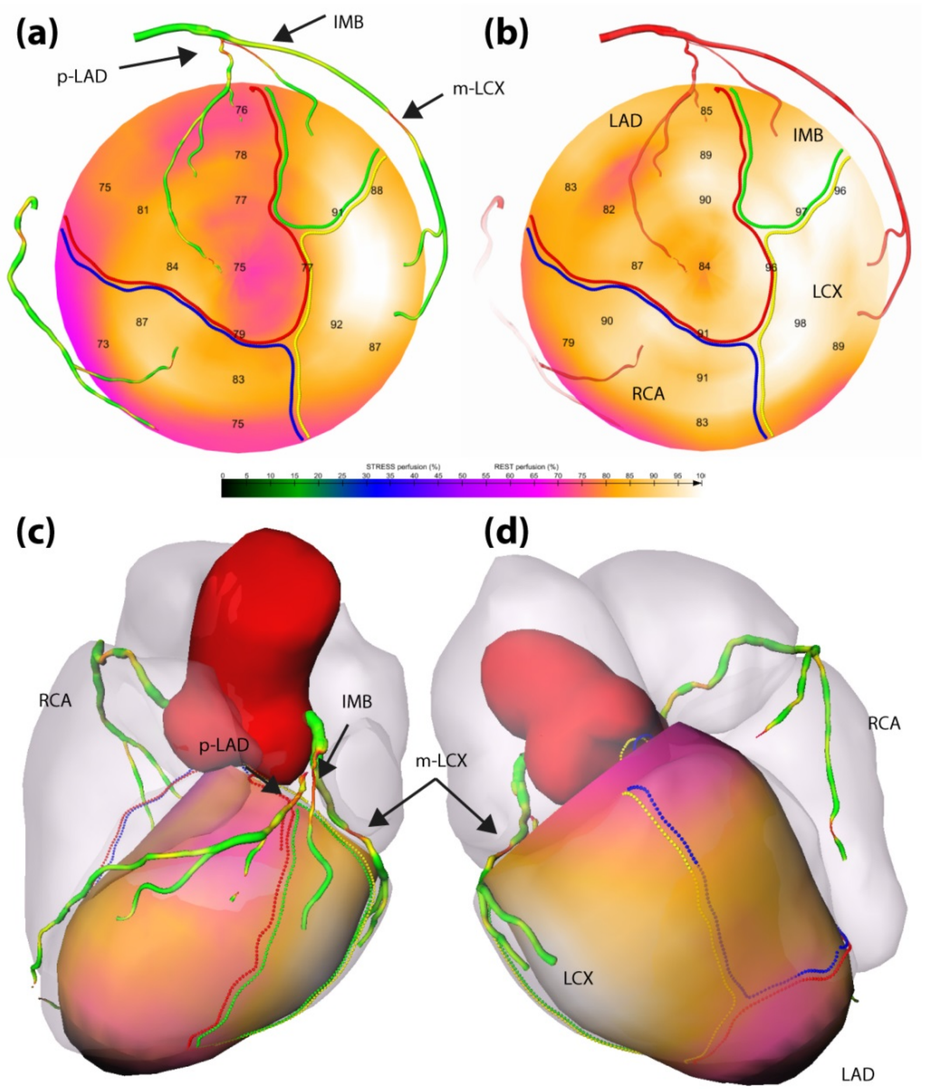

SMARTVis CTA + SPECT

Evaluation design

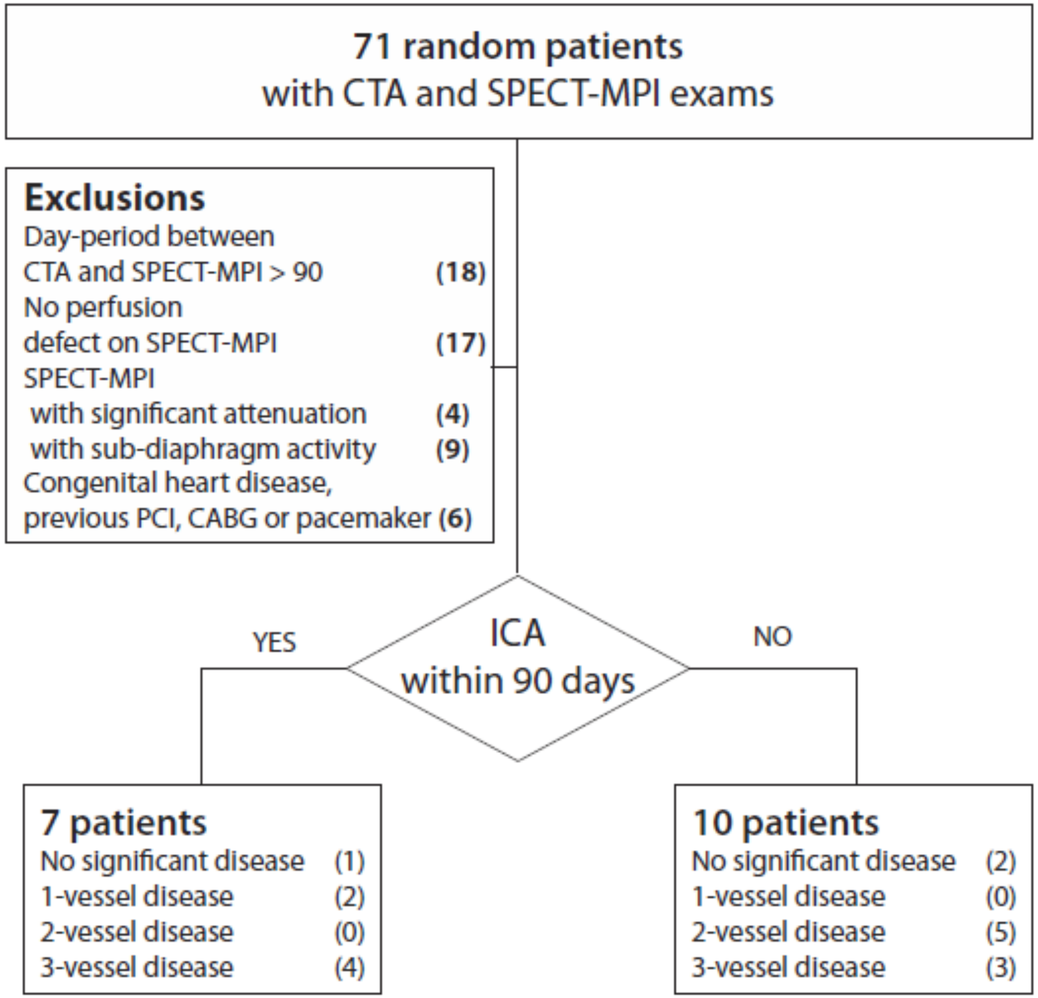

Figure 6.1: Patient's selection and exclusion criteria.

SMARTVis CTA + SPECT
Method

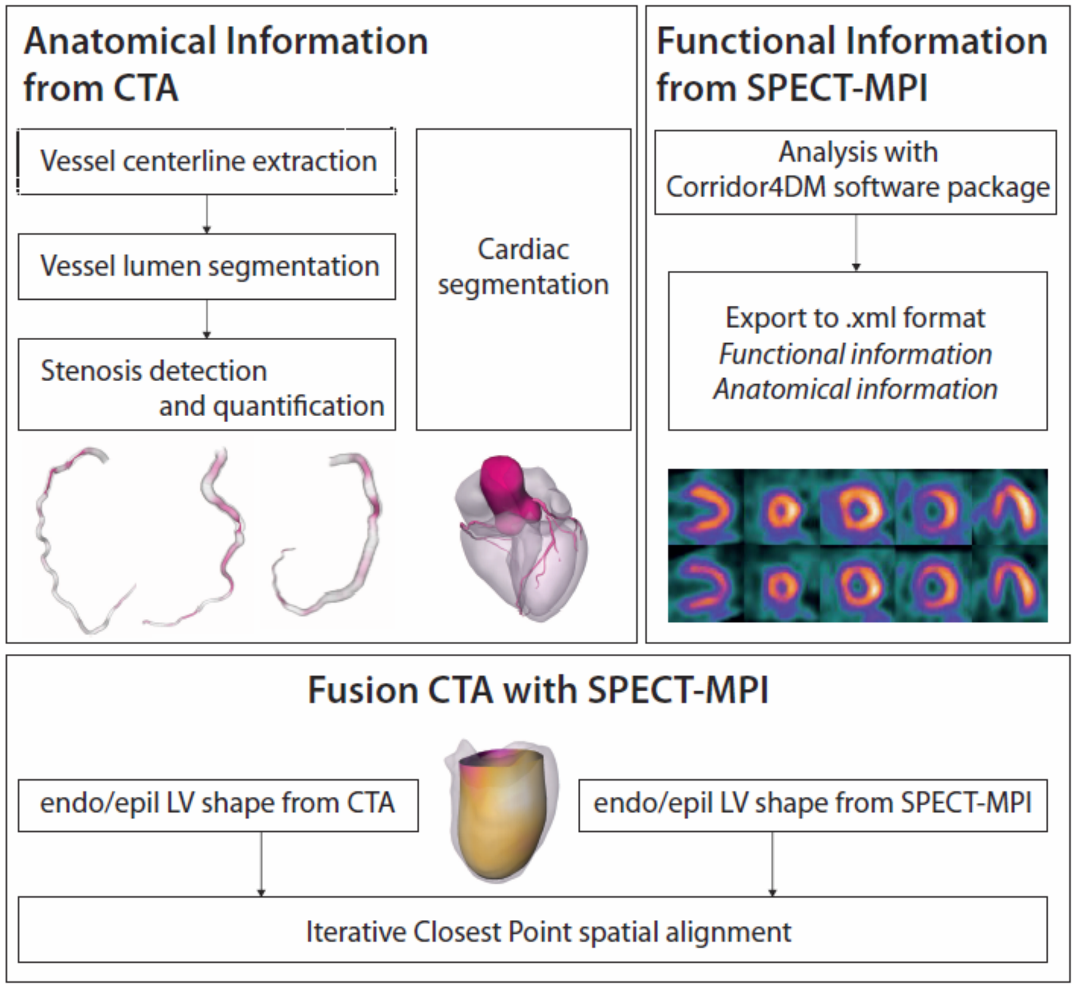

Figure 6.3: Overview of image processing performed on CTA and fusion of CTA/SPECT-MPI. The dashed box corresponds to semi-automatic process, while the solid boxes correspond to fully automatic processes. Coronary artery stenoses were detected and quantified on CTA using the method presented in Shahzad et al. (2012a); cardiac chamber shapes were obtained from CTA by applying method presented in Kirişli et al. (2010b). The SPECT-MPI left ventricle shape was automatically provided by the Corridor4DM software, as well as landmark points indicating the septal and apical positions. LV shapes and landmark points were subsequently used to align CTA and SPECT-MPI data by applying iterative closest point algorithm.

SMARTVis CTA + SPECT

Evaluation design

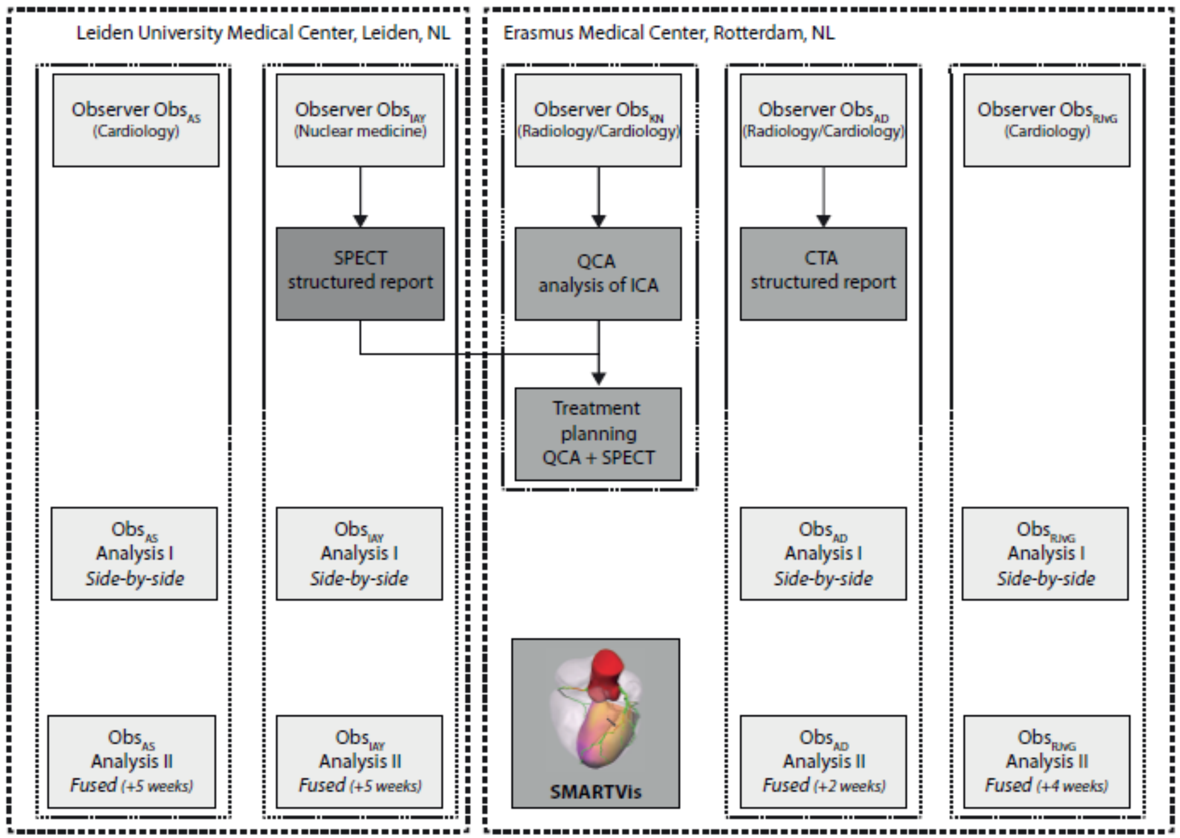

Figure 6.5: Overview of the evaluation study design. First, structured reports were created from CTA (ObsAD) and SPECT-MPI (ObsIAY), and QCA analysis was performed on the 7 available ICA. Treatment planning was performed for those 7 patients, based on QCA and SPECT-MPI findings. Second, four experts from two medical centers examined 17 patients with suspected CAD and performed 1) a side-by-side analysis, using structured CTA and SPECT-MPI reports, and 2) an integrated analysis, using the SMARTVis system in addition to the CTA and SPECT-MPI reports. Both analyses were performed with an interval of 2 to 5 weeks.

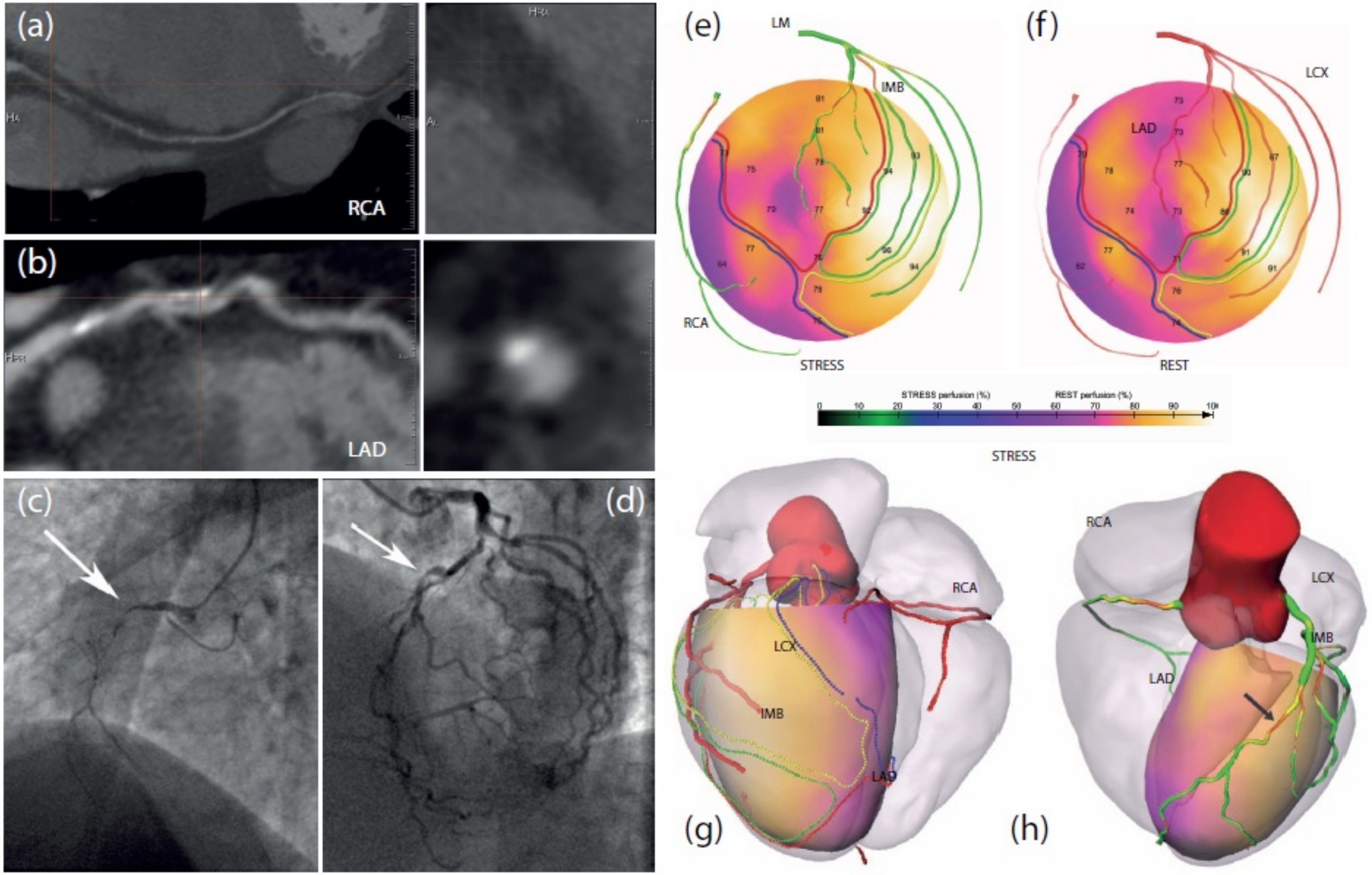

Figure 6.4: Example of patient 14 (male, 59 y.o.), who presents fixed perfusion defects in the inferior and anterior wall on SPECT-MPI and suspected triple-vessel disease on CTA. A complete occlusion was detected in the proximal RCA **(a)** and a moderate mixed plaque was detected in the middle LAD **(b)**. The QCA reveals a complete occlusion in proximal RCA **(c)** and a 50% stenosis in the middle LAD **(d)**. Comprehensive visualizations proposed in the SMARTVis system âĂŞ **(e)(f)** 2D stress and rest polar maps (PMAP) fused with projection of the coronary tree extracted from CTA. On the stress PMAP **(e)**, coronary arteries are color coded with the degree of stenosis; on the rest PMAP **(f)**, coronary arteries are coded with the distance to the epicardium: the more transparent the artery, the further it is from the epicardium. Patient-specific perfusion territories are also projected: LAD in red, LCX in yellow, MO in green and RCA in blue. **(g)(h)** 3D model of the heart and coronary artery tree extracted from CTA fused with 3D stress PMAP.

SMARTVis CTA + SPECT
Results

Table 6.3: Diagnostic performance for the side-by-side and fused CTA/SPECT-MPI analysis.

	Side-by-Side				Fused CTA/SPECT-MPI			
Patients with ICA (N=7)								
QCA/SPECT-MPI agreement	81%				91%			
Inter-observer agreement	66%				82%			
Sensitivity (4 observers)	80%	50%	60%	80%	100%	70%	80%	90%
Specificity (4 observers)	83%	100%	94%	83%	94%	100%	100%	83%
All patients (N=17)								
Inter-observer agreement	74%				84%			

SMARTVis

From a clinical point of view

- 2 clinical evaluation: CTA/MRI and CTA/SPECT-MPI

  Side by side analysis vs. fused analysis

  Correlate a coronary artery stenosis with a perfusion defect

  Detect which artery should undergo revascularization procedure?

  Comparison with QCA reference standard

- Conclusion: *Chapter 5 and 6 of this thesis*

+	–
Fused interpretation using SMARTVis	Side-by-side interpretation with mental integration

Analyse d'images médicales pour les maladies cardiovasculaires

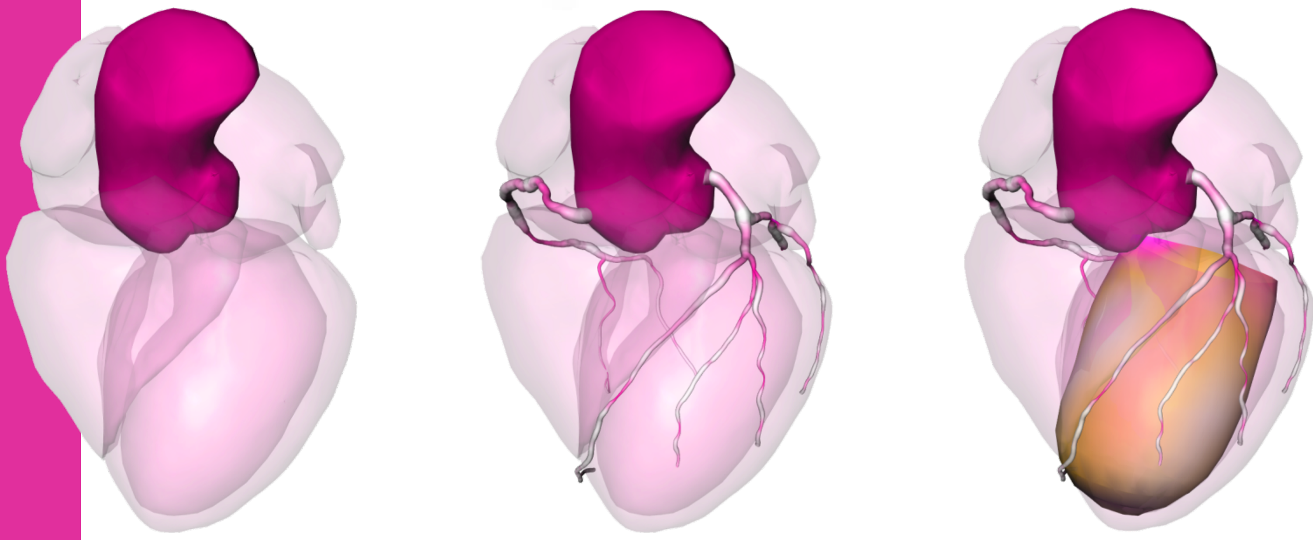

25 juin 2015
Workshop
VIVABRAIN
Paris, France

Dr. Hortense A. Kirisli
hortense.kirisli@gmail.com